

CEAW

METHOD of ANALYZING SEQUENTIAL
CONTROL ELEMENT ASSEMBLY
GROUP WITHDRAWAL EVENT for
ANALOG PROTECTED SYSTEMS

NOVEMBER, 1979

8007090 341

LEGAL NOTICE

THIS REPORT WAS PREPARED AS AN ACCOUNT OF WORK SPONSORED BY COMBUSTION ENGINEERING, INC. NEITHER COMBUSTION ENGINEERING NOR ANY PERSON ACTING ON ITS BEHALF:

A. MAKES ANY WARRANTY OR REPRESENTATION, EXPRESS OR IMPLIED INCLUDING THE WARRANTIES OF FITNESS FOR A PARTICULAR PURPOSE OR MERCHANTABILITY, WITH RESPECT TO THE ACCURACY, COMPLETENESS, OR USEFULNESS OF THE INFORMATION CONTAINED IN THIS REPORT, OR THAT THE USE OF ANY INFORMATION, APPARATUS, METHOD, OR PROCESS DISCLOSED IN THIS REPORT MAY NOT INFRINGE PRIVATELY OWNED RIGHTS; OR

B. ASSUMES ANY LIABILITIES WITH RESPECT TO THE USE OF, OR FOR DAMAGES RESULTING FROM THE USE OF, ANY INFORMATION, APPARATUS, METHOD OR PROCESS DISCLOSED IN THIS REPORT.

ABSTRACT

This report documents the new methods that can be used in analyzing the sequential CEA Group Withdrawal (CEAW) event for C-E's analog protected systems. The CEAW event is currently classified as requiring the Thermal Margin/Low Pressure (TM/LP) and the Axial Shape Index (ASI) trips to ensure that DNB and Centerline Temperature Melt (CTM) Specified Acceptable Fuel Design Limits (SAFDL's) are not exceeded. This document supports the reclassification of this event to a category where sufficient initial steady state thermal margin is build into DNB and Linear Heat Rate (LHR) Limiting Conditions for Operations (LCO's) to ensure that DNB and CTM SAFDL's are not exceeded.

The reclassification of this event is accomplished by relying on the High Power Trip (HPT) or the Variable High Power Trip (VHPT) and not the TM/LP and ASI trips to mitigate the consequences of this event. A detailed analysis has been performed to determine the initial conditions which cause the largest DNB and CTM margin degradation during the transient when only the HPT or the VHPT are credited.

TABLE OF CONTENTS

<u>SECTION</u>	<u>PAGE No.</u>
1. INTRODUCTION	1-1
2. DESCRIPTION OF TRANSIENT	2-1
3. CRITERIA OF ANALYSIS	3-1
4. INPUT PARAMETERS AND INITIAL CONDITIONS	4-1
5. METHOD OF ANALYSIS	5-1
5.1 REQUIRED OVERPOWER MARGIN ON DNBR	5-1
5.2 FUEL CENTERLINE TEMPERATURE MELT SAFDL	5-4
6. RESULTS	6-1
6.1 REQUIRED OVERPOWER MARGIN ON DNBR	6-1
6.2 FUEL CENTERLINE TEMPERATURE MELT SAFDL	6-7
7. CONSERVATISMS IN THE ANALYTICAL METHODS	7-1
7.1 CONSERVATISMS IN CALCULATION OF REQUIRED OVER POWER MARGIN ON DNBR	7-1
7.2 CONSERVATISMS IN CALCULATION OF FUEL CENTERLINE TEMPERATURE MELT SAFDL	7-3
8. CONCLUSIONS	8-1
9. REFERENCES	9-1
10. APPENDIX	A -1
METHODS USED TO DETERMINE EXCORE DETECTOR RESPONSES DURING A CEAW TRANSIENT	

LIST OF TABLES

<u>TABLE NO.</u>	<u>TITLE</u>	<u>PAGE</u>
4-1	Key Input Parameters Considered in the CEAW Event Analysis	4-4
6.1-1	Required Overpower Margin at 102% of Rated Power	6-10
6.1-2	Required Overpower Margin as a Function of ASI at 102% of Rated Thermal Power	6-11
6.1-3	Required Overpower Margin at 70% and 50% of Rated Thermal Power	6-12
6.1-4	Final Required Overpower Margin as a Function of ASI at 70% of Rated Thermal Power	6-13
6.1-5	Sequence of Events for CEA Withdrawal Event Initiated at 102% of Rated Power	6-14
6.1-6	Sequence of Events for CEA Withdrawal Event Initiated at 70% of Rated Power	6-15
6.1-7	Sequence of Events for CEA Withdrawal Event Initiated at 50% of Rated Power	6-16
6.1-8	Sequence of Events for CEA Withdrawal Event Initiated at HZP.	6-17
6.2-1	PLHGR as a Function of Power Level	6-18
7.1-1	Key Input Parameters Used in CEAW Event Initiated from 102% of Rated Power	7-5
7.1-2	Key Input Parameters Used in CEAW Event Initiated from 50% of Rated Power	7-6
7.1-3	Sequence of Events for CEA Withdrawal Event Initiated at 102% of Rated Power (Best estimate)	7-7
7.1-4	Sequence of Events for CEA Withdrawal Event Initiated at 50% of Rated Power (Best estimate)	7-8

LIST OF FIGURES

<u>FIGURE NO.</u>	<u>TITLE</u>	<u>PAGE</u>
4-1	Power Dependent Insertion Limit	4-5
5.1-1	Procedures Used to Determine DNBR Required Overpower Margin	5-6
5.2-1	Procedures for Calculating PLHGR	5-8
6.1-1	CEA Withdrawal Event from 102% Power - ROPM (DNBR) vs. CEA Reactivity Insertion Rate with Hgap Equal to []	6-19
6.1-2	CEA Withdrawal Event from 102% Power - ROPM (DNBR) vs. CEA Reactivity Insertion Rate with Hgap Equal to []	6-20
6.1-3	CEA Withdrawal Event from 102% Power - ROPM (DNBR) vs. CEA Reactivity Insertion Rate with Hgap Equal to []	6-21
6.1-4	CEA Withdrawal Event from 102% Power - ROPM (DNBR) vs. CEA Reactivity Insertion Rate with Hgap Equal to []	6-22
6.1-5	CEA Withdrawal Event from 102% Power ROPM (DNBR) vs. CEA Reactivity Insertion Rate and Hgap	6-23
6.1-6	CEA Withdrawal Event from 102% Power ROPM (DNBR) vs. CEA Reactivity Insertion with MTC Equal to []	6-24
6.1-7	CEA Withdrawal Event from 102% Power ROPM (DNBR) vs. CEA Reactivity Insertion Rate with MTC Equal to []	6-25
6.1-8	CEA Withdrawal Event from 102% Power - Axial Shape Index Shift vs. Initial Axial Shape Index	6-26
6.1-9	CEA Withdrawal Event from 102% Power - Integrated Radial Decrease vs. Initial Axial Shape Index	6-27
6.1-10	CEA Withdrawal Event from 102% Power - Penalty Factor on DNBR ROPM vs. Initial Axial Shape Index	6-28
6.1-11	CEA Withdrawal Event from 102% Power ROPM (DNB) vs. Initial Axial Shape Index	6-29
6.1-12	CEA Withdrawal Event from 70% Power ROPM (DNBR) vs. CEA Reactivity Insertion Rate	6-30

LIST OF FIGURES (CONTINUED)

<u>FIGURE NO.</u>	<u>TITLE</u>	<u>PAGE</u>
6.1-13	CEA Withdrawal Event from 50% Power ROPM (DNBR) vs. CEA Reactivity Insertion Rate	6-31
6.1-14	CEA Withdrawal Event from 70% Power Axial Shape Index Shift vs. Initial Axial Shape Index	6-32
6.1-15	CEA Withdrawal Event from 70% Power - Integrated Radial Decrease vs. Initial Axial Shape Index	6-33
6.1-16	CEA Withdrawal Event from 70% Power - Penalty Factor on DNBR ROPM vs. Initial Axial Shape Index	6-34
6.1-17	CEA Withdrawal Event from 70% Power ROPM (DNB) vs. Initial Axial Shape Index	6-35
6.1-18	CEA Withdrawal Event from 50% Power Axial Shape Index Shift vs. Initial Axial Shape Index	6-36
6.1-19	CEA Withdrawal Event from 50% Power - Integrated Radial Decrease vs. Initial Axial Shape Index	6-37
6.1-20	CEA Withdrawal Event from 50% Power - Penalty Factor on DNBR ROPM vs. Initial Axial Shape Index	6-38
6.1-21	CEA Withdrawal Event - Required Overpower Margin vs. Initial Power Level	6-39
6.1-22	CEA Withdrawal Event from 102% Power - Core Power vs. Time	6-40
6.1-23	CEA Withdrawal Event from 102% Power - Core Average Heat Flux vs. Time	6-41
6.1-24	CEA Withdrawal Event from 102% Power - RCS Temperatures vs. Time	6-42
6.1-25	CEA Withdrawal Event from 102% Power RCS Pressure vs. Time	6-43
6.1-26	CEA Withdrawal Event from 70% Power Core Power vs. Time	6-44
6.1-27	CEA Withdrawal Event from 70% Power Core Average Heat Flux vs. Time	6-45
6.1-28	CEA Withdrawal Event from 70% Power RCS Temperatures vs. Time	6-46
6.1-29	CEA Withdrawal Event from 70% Power RCS Pressure vs. Time	6-47

LIST OF FIGURES (CONTINUED)

<u>FIGURE NO.</u>	<u>TITLE</u>	<u>PAGE</u>
6.1-30	CEA Withdrawal Event from 50% Power Core Power vs. Time	6-48
6.1-31	CEA Withdrawal Event from 50% Power Core Average Heat Flux vs. Time	6-49
6.1-32	CEA Withdrawal Event from 50% Power RCS Temperatures vs. Time	6-50
6.1-33	CEA Withdrawal Event from 50% Power RCS Pressure vs. Time	6-51
6.1-34	CEA Withdrawal Event from HZP Power Core Power vs. Time	6-52
6.1-35	CEA Withdrawal Event from HZP Power Core Average Heat Flux vs. Time	6-53
6.1-36	CEA Withdrawal Event from HZP Power RCS Temperatures vs. Time	6-54
6.1-37	CEA Withdrawal Event from HZP Power RCS Pressure vs. Time	6-55
6.1-38	CEA Withdrawal Event from 102% Power Excore Detector Power vs. Time	6-56
6.1-39	CEA Withdrawal Event from 70% Power Excore Detector Power vs. Time	6-57
6.1-40	CEA Withdrawal Event from 50% Power Excore Detector Power vs. Time	6-58
6.2-1	CEA Withdrawal Event from 102% Power Peak Linear Heat Generation Rate vs. Gap Thermal Conductivity	6-59
6.2-2	CEA Withdrawal Event from 102% Power Peak Linear Heat Generation Rate vs. Initial Power Level	6-60
6.2-3	CEA Withdrawal Event From 102% Power Core Power vs. Time	6-61
6.2-4	CEA Withdrawal Event from 70% Power Core Power vs. Time	6-62
6.2-5	CEA Withdrawal Event from 50% Power Core Power vs. Time	6-63

LIST OF FIGURES (CONTINUED)

<u>FIGURE NO.</u>	<u>TITLE</u>	<u>PAGE</u>
6.2-6	CEA Withdrawal Event from HZP Core Power vs. Time	6-64
7.1-1	CEA Withdrawal Event from 102% Power Core Power vs. Time	7-9
7.1-2	CEA Withdrawal Event from 102% Power Core Average Heat Flux vs. Time	7-10
7.1-3	CEA Withdrawal Event from 102% Power RCS Temperatures vs. Time	7-11
7.1-4	CEA Withdrawal Event from 102% Power RCS Pressure vs. Time	7-12
7.1-5	CEA Withdrawal Event from 50% Power Core Power vs. Time	7-13
7.1-6	CEA Withdrawal Event from 50% Power Core Average Heat Flux vs. Time	7-14
7.1-7	CEA Withdrawal Event from 50% Power RCS Temperatures vs. Time	7-15
7.1-8	CEA Withdrawal Event from 50% Power RCS Pressure vs. Time	7-16
7.2-1	CEA Withdrawal Event from 102% Power Core Power vs. Time	7-17
7.2-2	CEA Withdrawal Event from HZP Core Power vs. Time	7-18

LIST OF ACRONYMS AND ABBREVIATIONS

AOO	Anticipated Operational Occurrence (s)
ARO	All Rods Out
ASI	Axial Shape Index
AXPD	Axial Power Distribution
CEA	Control Element Assembly
CEAW	Control Element Assembly Withdrawal
CEAW rate	CEA Reactivity Insertion (withdrawal) Rate
CTM	Centerline Temperature Melt
DBE	Design Basis Event (s)
DNB	Departure from Nucleate Boiling
DNBR	Departure from Nucleate Boiling Ratio
F_A	Peaking Augmentation Factor
FP	Fractional Power Rise during the Transient
F_R	Integrated Radial Peak
FTC	Fuel Temperature Coefficient
F_{TILT}	Azimuthal Tilt Allowance
F_{xy}	Planar Radial Peak
F_Z	Axial Peak
H_{gap}	Gap Thermal Conductivity
HPT	High Power Trip
HZP	Hot Zero Power
LCO	Limiting Condition (s) for Operation
LHR	Linear Heat Rate
MTC	Moderator Temperature Coefficient
MWt	Megawatt (s), thermal
NSSS	Nuclear Steam Supply System (s)
PDIL	Power Dependent Insertion Limit

LIST OF ACRONYMS AND ABBREVIATIONS (CONTINUED)

PLCS.	Pressurizer Level Control System
PLHGR	Peak Linear Heat Generation Rate
PPCS	Pressurizer Pressure Control System
RCS	Reactor Coolant System
ROPM	Required Overpower Margin
RPS	Reactor Protective System
RSF	Rod Shadowing Factor
SAFDL	Specified Acceptable Fuel Design Limit (s)
T_C	Centerline Temperature
TM/LP	Thermal Margin Low Pressure
TSF	Temperature Shadowing (Attenuation) Factor
VHPT	Variable High Power Trip
ΔE	Integrated Energy Rise
ΔE_C	Centerline Energy Rise
$\Delta E_{H.S.}$	Integrated Energy Rise at Hot Spot
$\frac{\Delta FN}{q}$	Fractional Increase in 3-D Peak
F_{xy}	Planar Radial Peak

1. INTRODUCTION

The purpose of this report is to document the new methods which can be used in analyzing the Control Element Assembly Group Withdrawal (CEAW) event. The methods reported herein are applicable to Baltimore Gas and Electric's Calvert Cliffs Units I and II.

For Anticipated Operational Occurrences (AOO's) the DNB and Centerline Temperature Melt (CTM) Specified Acceptable Fuel Design Limits (SAFDL's) will not be violated provided:

1. The actuation of a Reactor Protective System (RPS) trip intervenes to ensure that SAFDL's are not exceeded, or
2. Sufficient initial margin is built in to ride through the transient without requiring a trip, or there is an RPS trip in combination with sufficient initial steady state margin to the DNB and CTM SAFDL's. This initial margin is provided by Limiting Conditions for Operations (LCO's) specified in the plant Technical Specifications.

As stated in CENPD-199-P (Reference 1), the CEAW event has been classified as an AOO requiring the actuation of an RPS trip. Specifically, the Thermal Margin/Low Pressure Trip prevents exceeding the DNB SAFDL and the Axial Shape Index (ASI) trip prevents exceeding the CTM SAFDL. Thus, in the past this event was analyzed to calculate the pressure bias input to the TM/LP trip to ensure that DNB SAFDL was not exceeded and to confirm that power input to both the TM/LP and axial shape index trips was conservative.

The pressure bias term accounted for the margin degradation from the time a TM/LP trip signal is actuated to the time of transient minimum DNBR. The bias term accounts for temperature and pressure differences between the actual system temperatures and pressures at the time a trip setpoint is encountered and those at the time of minimum DNBR. The pressure bias factor along with conservative power, temperature and pressure input to the TM/LP trip ensured that DNB SAFDL would not be exceeded. The CTM SAFDL would not be exceeded due to the actuation of the ASI trip utilizing conservatively high power input signals.

The new method and its consequences, which are described in detail in this document, justify reclassification of this event from the category requiring the action of TM/LP and ASI trips to the category where sufficient initial steady state thermal margin is built into the DNB and LHR LCO's to ensure that SAFDL's are not exceeded. Credit is taken only for the High Power Trip (HPT) and the Variable High Power Trip (VHPT). The new method is based on calculating the Required Overpower Margin (ROPM) that must be provided by adherence to the LCO's. Actuation of the HPT or the VHPT is then sufficient to prevent violation of SAFDL's in lieu of including a pressure bias component in the TM/LP trip algorithm. It should be noted that the bias term for the TM/LP is still determined for other transients as described in Reference 1.

In summary, this document describes and justifies the following:

1. The new methods and procedures used to calculate the DNB and LHR ROPM's.
2. The results of the detailed analysis, including sensitivity studies for key parameters, which establish conservative estimates of DNB and CTM margin degradation.

2. DESCRIPTION OF TRANSIENT

To understand what the key parameters are, a brief description of the transient follows:

A CEA withdrawal event is assumed to occur as a result of a failure in either the Control Element Drive Mechanism Control System (CEDMCS) or the Reactor Regulating System (RRS).

The withdrawal of CEA's inserts positive reactivity which increases the core power and heat flux. The increases in the core power and heat flux in turn increase the Reactor Coolant System (RCS) temperatures and pressure. The withdrawal of CEA's can also shift the axial power distribution toward the top of the core. Also, as the CEA's are withdrawn, the integrated radial peaks (F_R) decrease.

The withdrawal of CEA's generally decalibrates the flux power signal measured by the excore detectors. These detectors provide power input to the RPS. However, the magnitude of the decalibration due to CEA motion is offset by the decreased neutron flux attenuation (temperature shadowing) due to increases in the inlet coolant temperature. A discussion of the excore detector responses during a CEAW event is given in the Appendix.

The calculation of margin degradation during this event accounts for the following:

1. increases in core power
2. increases in core heat flux
3. increases in RCS temperatures
4. increases in RCS pressure
5. decreases in core mass flow rate (due to density changes)
6. changes in axial power distribution and integrated radial peaks.

Since the overall margin degradation during this event depends on the combined effects of changes in all of the above mentioned parameters, a detailed sensitivity study on key parameters was performed to establish a combination of parameters which produces maximum margin degradation.

3. CRITERIA OF ANALYSIS

The CEAW event is classified as an AOC; hence the following criteria are applicable.

- i) Minimum Transient DNBR \geq DNBR SAFDL based on CE-1 correlation⁽¹⁾
- ii) Maximum Fuel Centerline Temperature at Melt⁽²⁾ $< 5080^{\circ}\text{F} - \frac{280 \times \text{Burnup (MWD/MT)}}{50,000 \text{ (MWD/MT)}}$

- NOTES: 1. CE-1 DNBR shall have a minimum allowable limit corresponding to a 95% probability at a 95% confidence level that DNB will not occur. In this study a DNBR of 1.19 was used.
2. The fuel centerline melt SAFDL is not exceeded if the Peak Linear Heat Generation Rate (PLHGR) does not exceed a steady state limit. In this study a limit of 21 KW/ft was used. For some CEAW cases, the reactor power rises rapidly for a very short period of time before the power transient is terminated. Hence, for these CEAW cases where the steady state limit of 21 KW/ft is exceeded, the total energy generated and the corresponding temperature rise at the hot spot are calculated for the duration of transient to demonstrate that fuel centerline temperatures do not exceed UO_2 melt temperatures. That is, for rapid power spikes of short duration a time at power is more significant than the peak linear heat generation rate achieved.

4. INPUT PARAMETERS AND INITIAL CONDITIONS

Table 4-1 presents the range of initial conditions considered in this analysis. The reactor state parameters of primary importance in calculating the margin degradation are: 1) CEA withdrawal rate* (i.e., reactivity insertion rate), 2) gap thermal conductivity (H_{gap}), 3) initial power level, 4) flux power level determined from excore detector response during the transient, 5) the Moderator Temperature Coefficient (MTC) of reactivity, and 6) axial power distribution and planar and integrated radial peaking factor changes during the transient.

A parametric analysis in H_{gap} , CEA withdrawal (or reactivity insertion) rate and the MTC was performed to determine the combination of these parameters which produces the largest margin degradation during the event. The analysis was performed at various power levels to obtain the margin degradation during the transient as a function of initial power level. The excore detector responses for each initial power level analyzed were based on the CEA insertions allowed by the Power Dependent Insertion Limit (PDIL) (See Figure 4-1) at the selected power level, the changes in CEA position prior to trip, and the corresponding rod shadowing and temperature attenuation (shadowing) factors. The methods used to determine the excore detector responses during the transient are presented in the Appendix.

Other input parameters of importance are the Fuel Temperature Coefficient (FTC) of reactivity and the initial and final axial power distributions. A FTC corresponding to beginning of life conditions was used in the analysis, since this FTC causes the least amount of negative

*Note: The term CEA withdrawal rate and CEA reactivity insertion rate are used interchangeably in this report.

reactivity feedback to offset the transient increases in core power and heat flux. The uncertainty on the FTC used in the analyses is shown in Table 4.1 and is the same as quoted in previous reload licensing submittals.

For the CEAW cases where the combinations of parameters result in a reactor trip, the scram reactivity versus insertion characteristics assumed were those associated with a core average axial power distribution peaked at the bottom of the core. The bottom peaked shape assumed is characterized by a shape index of []. The scram reactivity versus insertion characteristics associated with this bottom peaked shape minimize the amount of negative reactivity inserted during the initial portion of the scram following a reactor trip. This, in turn, maximizes the time required to turn around the transient power, heat flux and coolant temperature increases. However, it should be noted that a bottom peaked shape is used only to determine the NSSS response during the event. These responses were then combined with the axial power distributions shifted toward the top of the core. Initial axial power distributions allowed within the positive and negative shape index extremes of the DNB LCO band were evaluated to obtain the margin degradation as a function of shape index.

All control systems except the Pressurizer Pressure Control System (PPCS) and Pressurizer Level Control System (PLCS) were assumed to be in manual mode. These are the most adverse operating modes for this event. The PPCS and PLCS were assumed to be in the automatic mode since the actuation of these systems minimizes the rise in the coolant system pressure. The net effect is to delay a reactor trip until a High Power trip is initiated. This allows the transient increases in power, heat flux and coolant temperature to proceed for a longer period of time.

In addition, minimizing the pressure increase is conservative in the margin degradation calculations since increases in pressure would offset some of the DNB margin degradation caused by the increases in the core heat flux and the coolant temperatures.

TABLE 4-1

KEY INPUT PARAMETERS CONSIDERED IN THE CEAW EVENT ANALYSIS

<u>Parameters</u>	<u>Units</u>	<u>Range of Values</u>
Initial Power Level	% of 2710 MWt	0 to 102
Initial Coolant Temperature	°F	532 to 550*
Initial Coolant System Pressure	psia	2200 ⁺
Initial Core Mass Velocity	$\times 10^6$ lbm/hr-ft ²	2.53 ⁺
Moderator Temperature Coefficient	$\times 10^{-4}$ $\Delta\rho/^\circ\text{F}$	+0.5 to -2.5
Fuel Temperature Coefficient Uncertainty	%	-15.0 ⁺
Gap Thermal Conductivity	BTU/hr-ft ² -°F	[...]
Axial Shape Index for Scram Characteristics	asiu	[+0.54] ⁺
CEA Differential Worth	$\times 10^{-4}$ $\Delta\rho/\text{inch}$	[...]
CEA Withdrawal Speed	inches/minute	30.0
CEA Worth at Trip:		
100%	% $\Delta\rho$	$\geq -4.6^+$
All other power levels	% $\Delta\rho$	$\geq -3.4^+$
High Power Trip Analysis Setpoint	% of 2710 MWt	112.0
Variable High Power Trip Analysis Setpoint	% above initial power level	10.0
Integrated Radial Peaking Factor		1.65 to 2.6**
Maximum 2D-Peak, F_{xy}^{***}		2.6 ⁺
Maximum Axial Peak, F_z^{***}		2.0 ⁺
Augmentation Factor, F_A^{***}		1.07 ⁺
Uncertainty, F_{UNC}^{***}		1.10
Tilt (HZP), F_T^{***}		1.10
Temperature Shadowing Factor	%Power/°F	[...]

* Initial T_{in} values used are maximum for a given power level based on the Tave Program.

** The integrated radial peaking factors used are the maximum for a given power level based on the CEA insertions allowed by POIL at that power level.

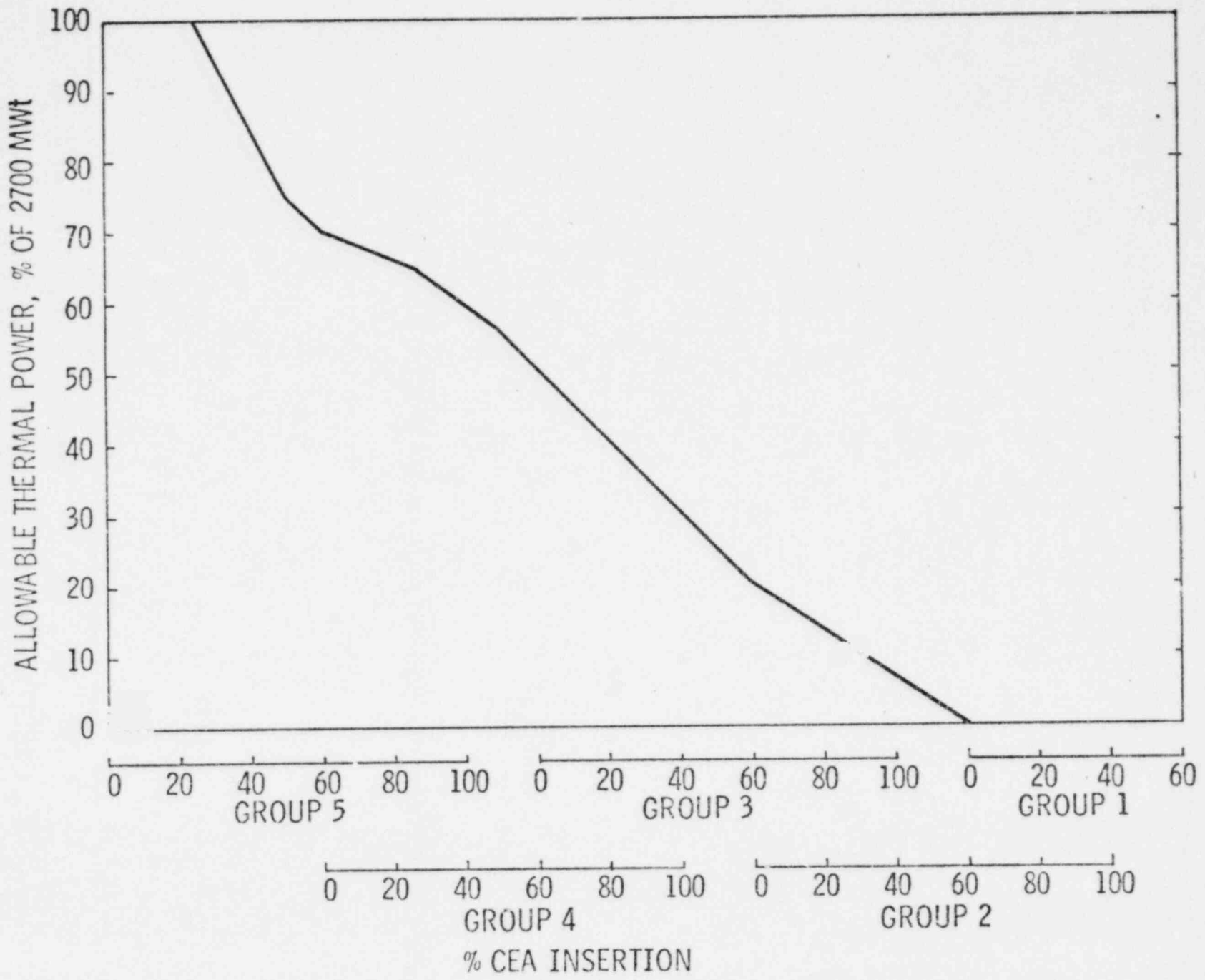
*** Values used in calculating maximum fuel centerline temperatures and minimum DNBR for CEAW event initiated at HZP.

+ The initial values of these parameters were selected to be those which produce the maximum margin degradation.

POWER DEPENDENT INSERTION LIMIT

4-5

Figure 4-1



5. METHOD OF ANALYSIS

The Nuclear Steam Supply System (NSSS) response to a CEA group withdrawal event was simulated using the digital computer code CESEC, described in CENPD-107 (Reference 2). The thermal hydraulic design code TORC described in CENPD-162-P (Reference 3) was used to calculate the thermal margin degradation during the transient. The LHR margin degradation was calculated using the procedures and methods discussed in Section 5.2.

5.1 REQUIRED OVERPOWER MARGIN ON DNBR

The calculation procedures used in the analysis to determine DNBR ROM are presented in Figure 5.1-1. This procedure consists of:

1. Simulation of the CEAW transient using CESEC to determine the heat flux, coolant system temperatures and the coolant system pressures during the event. The key input parameters are discussed in Section 4.
2. A set of TORC cases are run to determine the time of minimum DNBR. Input to TORC are the time dependent values of heat flux, T_{in} , pressure and core mass flow rate predicted by CESEC. Other input parameters are integrated radial peak and axial power distribution.
3. A TORC case is run to determine the rod average power at which the fuel design limit on DNBR is reached for the

initial steady state system parameters. This value of power is designated B_1 .

4. The heat flux, inlet temperature, pressure and core mass flow at the time of minimum DNBR determined in step 2 are used in conjunction with initial value of integrated radial peak and axial power distribution to obtain a power at which the fuel design limit on DNBR is reached for the transient conditions. This power is designated B_2 .
5. The Required Overpower Margin ($ROPM_1$) (i.e., margin degradation) is computed as; $ROPM_1 = \frac{B_1}{B_2} \times 100\%$.
6. The QUIX code (Reference 4) is used to simulate a CEAW event to determine the axial power distribution (AXPD) changes and the decrease in the integrated radial peak. The input to QUIX are, 1) the transient variations in power and coolant temperatures predicted by CESEC, 2) the CEA bank worth, 3) CEA bank configuration-dependent rod shadowing factors, 4) CEA bank configuration-dependent radial peaking factors, 5) allowed CEA configuration at the initial power level based on the PDIL, and 6) shape annealing functions. The code calculates the initial and time dependent axial power distributions, radial peaking factors, ex-core indicated power, and shape index accounting for the transient variations in the xenon distributions and feed back effects.
7. Determine the margin loss at the time of minimum DNBR determined in Step 2 due to the axial power shape change and the margin gain due to the decrease in the radial peak for the range of ASI allowed by the DNB LCO band. The sum of these two components provides a net penalty factor, B_3 , on the ROPM at each axial shape index allowed by the DNB LCO band. The penalty factor, B_3 , is calculated from the following relationship:

This section describes C-E proprietary methods used in the analysis of the net penalty factor, B_3 , on the Required Overpower Margin.

8. Calculate the total DNB margin degradation as a function of initial shape index from the relation: []
9. For CEAW event initiated from Hot Zero Power (HZP) calculate the transient minimum DNBR, using the maximum value of integrated radial peak, a conservative AXPD and the maximum heat flux predicted by CESEC, to demonstrate that DNB SAFDL is not exceeded.

5.2 FUEL CENTERLINE TEMPERATURE MELT SAFDL

The procedures used to ensure that the fuel centerline melt SAFDL is not exceeded are displayed schematically in Figure 5.2-1. These procedures are as follows:

1. Simulate the CEAW transient with CESEC to obtain the fractional power rise during the event.
2. The fractional power rise obtained in the previous step is used along with equation 5.2-1 to calculate the Peak KW/ft during the event.

$$\text{PLHGR} = \text{PLHGR}_I + \Delta\text{PLHGR} = \text{PLHGR}_I \times (1 + \text{FP}) \times (1 + \Delta F_q^N) \quad \text{Equation 5.2-1}$$

where:

PLHGR = Peak Linear Heat Generation Rate during the event

PLHGR_I = Initial Peak Linear Heat Generation Rate allowed by the KW/ft LCO, including all uncertainties.

ΔPLHGR = Change in PLHGR due to power increases and power distribution changes.

FP = Fractional Power rise during the event.

ΔF_q^N = Fractional Increase in 3-D peak during the event.

3. The maximum centerline temperatures (T_{CL}) are calculated for the CEAW cases which exceed the steady state limit of 21 KW/ft to demonstrate that the UO_2 melt temperatures are not exceeded for high LHR's of short duration. The procedure to calculate the fuel centerline temperatures (T_{CL}) consists of the following steps:
 - a. Calculate the average integrated energy rise (ΔE) during the transient based on the power excursion predicted by CESEC.

- b. Calculate the energy rise at the hot spot using equation 4.2-1.

$$\Delta E_{H.S} = \Delta E \times F_{xy} \times F_Z \times F_A \times F_T \times F_{UNC} \text{ - Equation 4.2-1}$$

where:

ΔE = average energy rise

$\Delta E_{H.S}$ = Energy rise at hot spot

F_{xy} = Maximum 2-D Peak during transient

F_Z = Maximum Axial Peak during transient

F_A = Augmentation Factor (taken to be maximum at top of core)

F_T = Azimuthal Tilt Allowance

F_{UNC} = Uncertainty (on local peaking and power)

Since no credit is taken for heat transfer out of the fuel, the energy rise at the hot spot is equal to the centerline energy rise (ΔE_Q). Hence $\Delta E_Q = \Delta E_{H.S}$

- c. Obtain the centerline temperature rise (ΔT_Q) corresponding to the centerline energy rise by integrating as a function of temperature the specific properties of UO_2 described in Reference 5, assuming no heat transfer out of the fuel.
- d. Calculate maximum centerline temperature from:

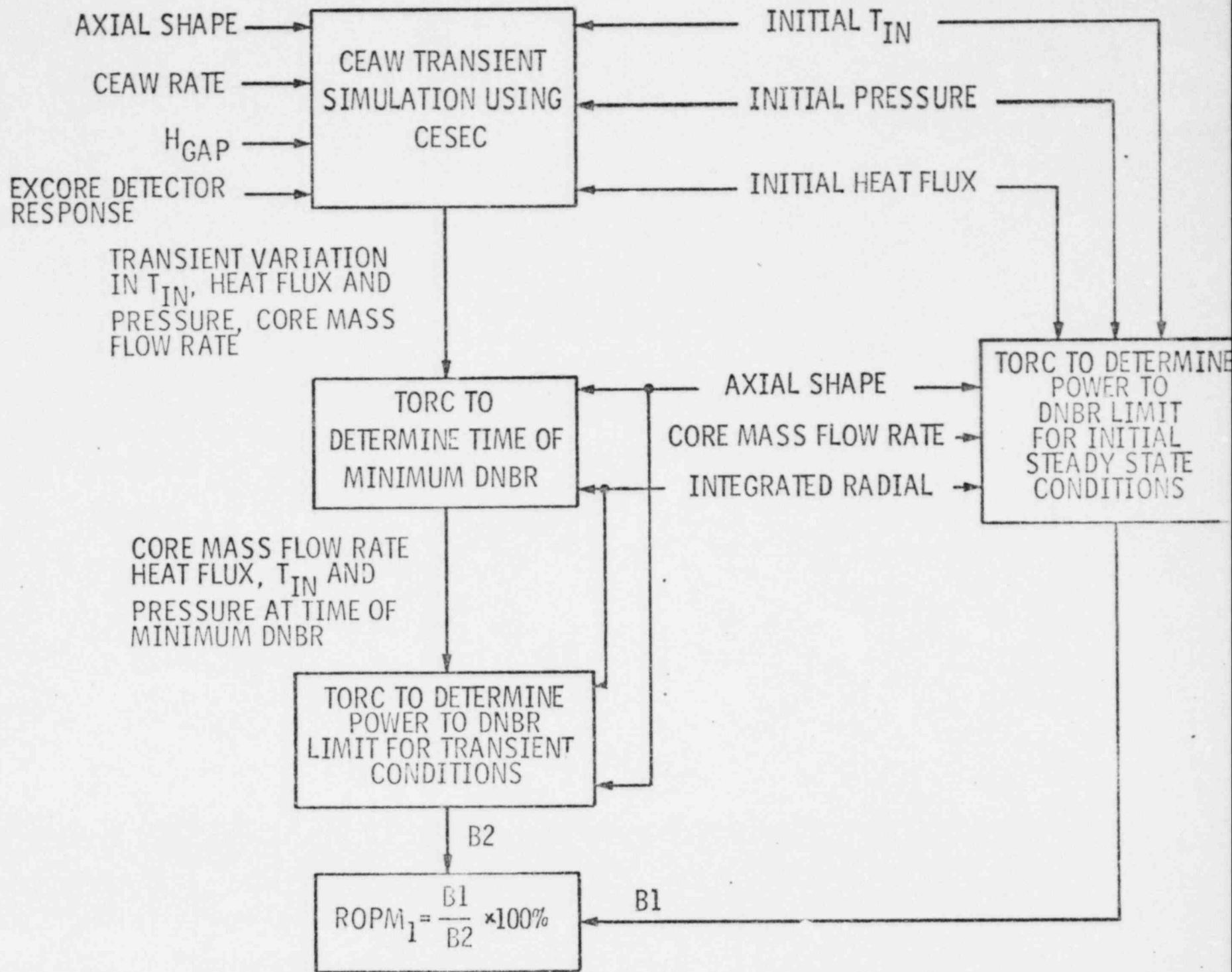
$$T_Q^{\max} = T_Q^I + \Delta T_Q$$

where:

T_Q^{\max} = Maximum centerline temperature

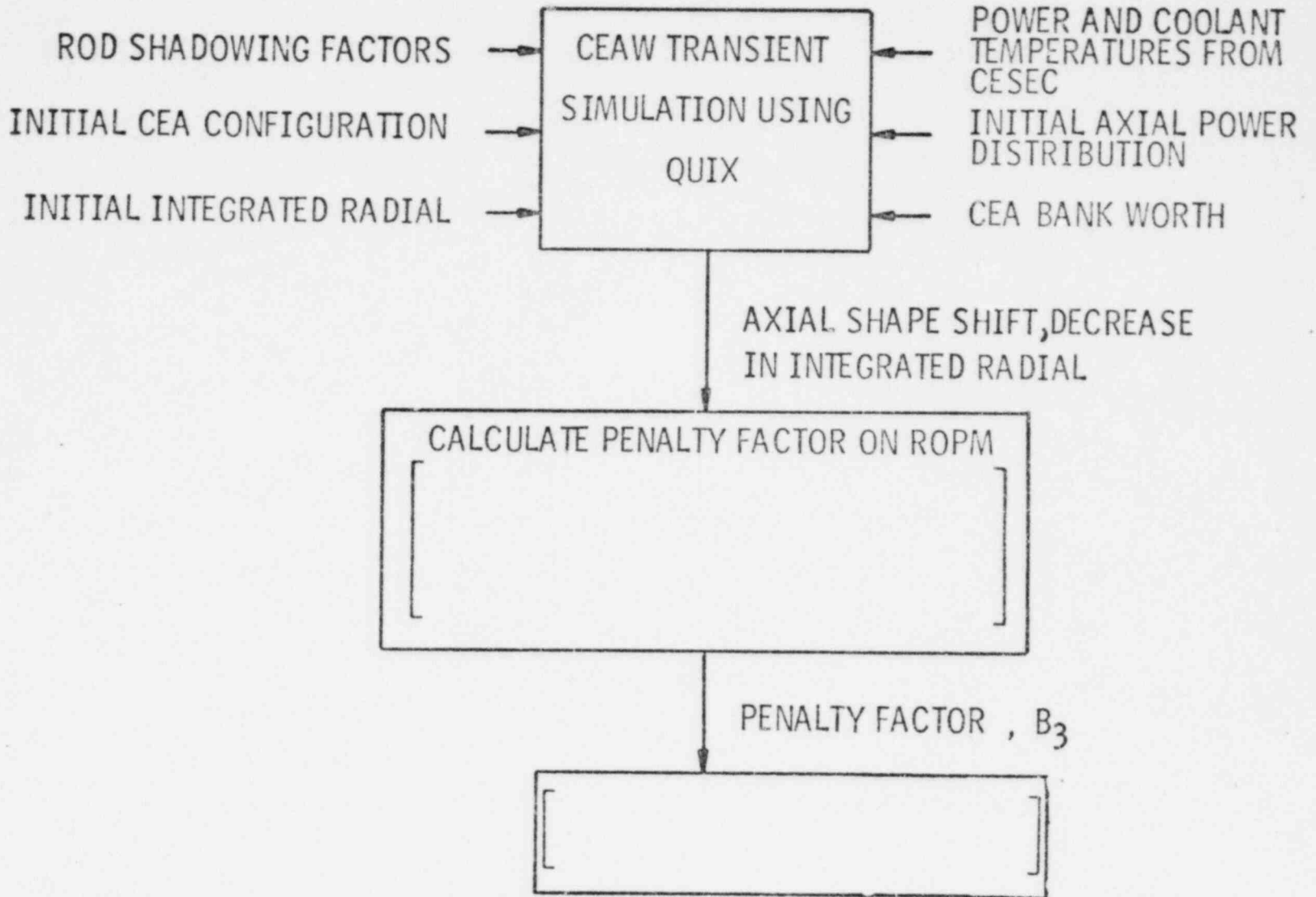
T_Q^I = Initial centerline temperature

ΔT_Q = Centerline temperature rise obtained in step c.



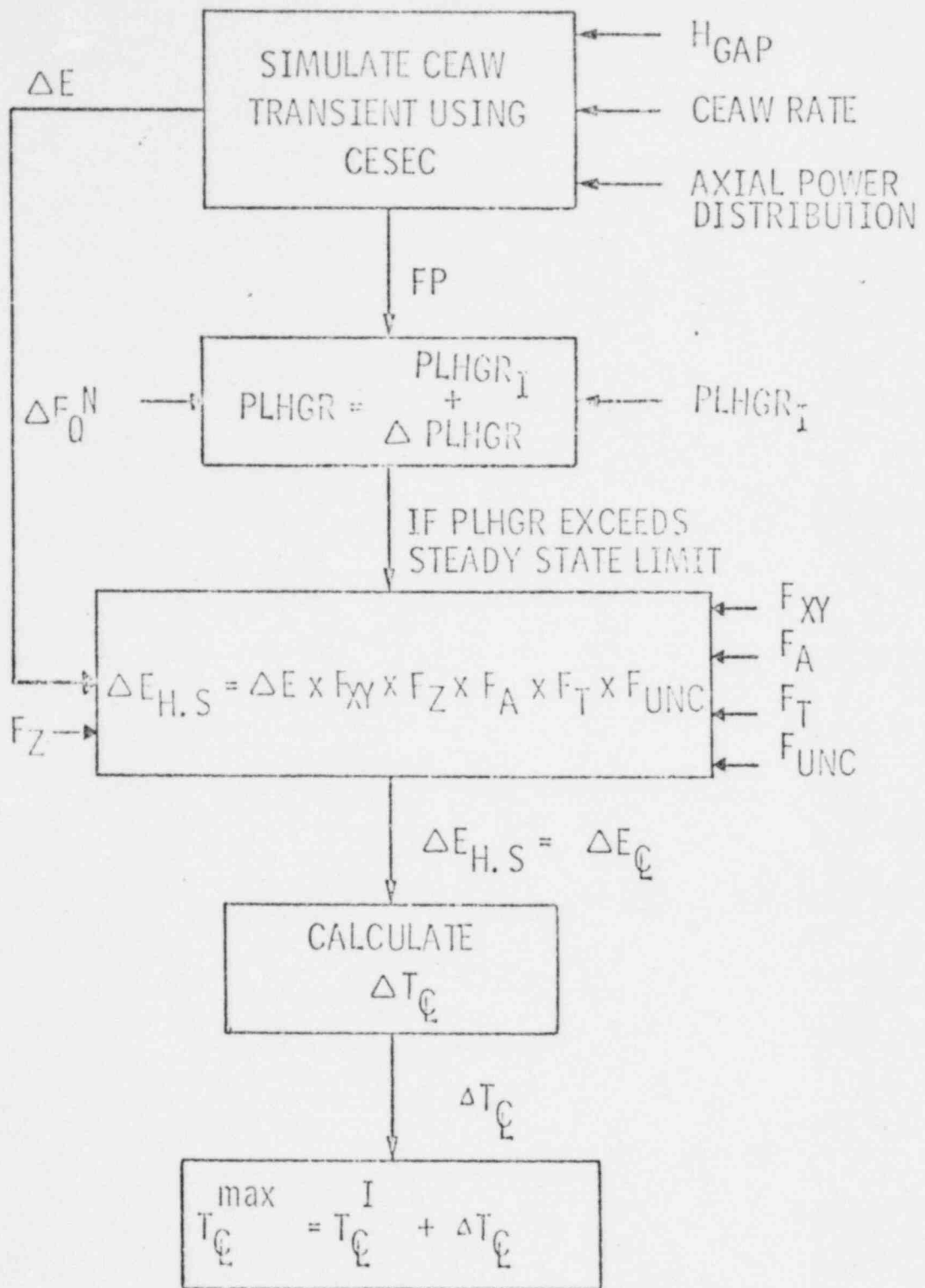
PROCEDURES USED TO DETERMINE DNBR REQUIRED OVER POWER MARGIN

FIGURE 5.1-1



PROCEDURES USED TO DETERMINE DNBR
 REQUIRED OVERPOWER MARGIN (Cont'd)

Figure
 5.1-1



PROCEDURES FOR CALCULATING PLHGR

FIGURE 5.2-1

6. RESULTS

The purpose of this section is to discuss the results of the parametric analysis performed to establish limiting combinations of parameters and to display values of the maximum DNBR and peak linear heat generation rate ROPM's obtained.

6.1 REQUIRED OVER POWER MARGIN ON DNBR

The results of the parametric analysis in CEA reactivity insertion rate and H_{gap} with a constant MTC of [] $\Delta\rho/^\circ\text{F}$ are presented in Figures 6.1-1 to 6.1-4. These figures present the results for the CEAW cases which initiated a reactor trip and the cases which did not initiate a reactor trip. The highest ROPM is obtained for [

] The ROPM is highest for this case because the inlet temperature is [] and the RCS pressure [] at the time of minimum DNBR than for cases which [

]. The core power and heat flux also achieve a new [] steady state value, but [

]. This occurs because of the [] coolant temperatures and leads to the []].

This causes the [

]

Figure 6.1-5 presents the ROPM for the [

] The results are also tabulated in Table 6.1-1 for the CEAW rates that produced the maximum ROPM for each of the

H_{gap} values analyzed. As seen from the Table [

]

A similar study in CEAW rate and H_{gap} was performed with an MTC of [] $\Delta\rho/^\circ\text{F}$. Figure 6.1-6 presents the results of this parametric analysis. The results indicate that the maximum ROPM for cases with an MTC of [] $\Delta\rho/^\circ\text{F}$ is lower than the ROPM's obtained from cases with an MTC of [] $\Delta\rho/^\circ\text{F}$. This occurs because with an MTC of [] $\Delta\rho/^\circ\text{F}$, [

] The larger positive reactivity insertion further accelerates the core power and coolant temperature rise. The faster increase in coolant temperatures in combination with [

] This occurs even for CEAW reactivity insertion rates as low as [] $\Delta\rho/\text{inch}$.

An analysis was also performed with an MTC of [] $\Delta\rho/^\circ\text{F}$. The results presented in Figure 6.1-7 indicate that the transient is self limiting because the increase in coolant temperature in combination with the [] retards the power, heat flux and temperature increases. Hence, with [] the power rise, coolant temperature rise and heat flux increase are much smaller than with [] Thus, the margin degradation is also lower for more [] The net result of the

parametric study is that [

] However, there is [

] Instead there is a [

] which produce the limiting case results.

The ROPM quoted previously (see Table 6.1-1) for the limiting CEAW event initiated at 102% of rated thermal power does not account for any axial power distribution shift (AXPD) and the associated decrease in the integrated radial peak (F_R). A detailed analysis was performed to determine the net ROPM change due to the axial shape shift and the decrease in F_R as a function of initial axial power distribution. Figure 6.1-8 presents the axial shape shift as a function of initial AXP. Figure 6.1-9 displays the corresponding decreases in integrated radial peak. Both the axial shape shift and the initial AXP are characterized by axial shape indices. The net penalty factor, B_3 , as a function of initial Axial Shape Index is given in Figure 6.1-10.

The results of the analysis indicate that [] axial shapes cause the maximum axial peak shift and thus result in the largest penalty factor. The results also indicate that for a CEAW event initiated at 102% of rated power with an axial shape index more [

] and the penalty factors shown in Figure 6.1-10 are combined with ROPM quoted previously in Table 6.1-1 to obtain the total DNB margin degradation as a function of initial ASI. Table 6.1-2 and Figure 6.1-11 presents the final ROPM as a function of initial ASI at 102% of rated power.

The results of the parametric analysis in CEA reactivity insertion rate, MTC and H_{gap} and initial axial power distribution at 102% of rated power indicates the following:

1. [This section describes C-E proprietary methods used in the analysis of ROPM.]

2. For the CEAW event initiated at 102% of rated power, the above occurs for a []

].

3. [] MTC's result in self limiting CEAW events, []

] This means []

]

4. [$\Delta\rho/^\circ\text{F}$ produce a reactor trip]

]

5. A net penalty factor of [] power at an ASI of [] has to be applied to the ROPM to account for the margin change due to axial shape shift and the decrease in the integrated radial peak. However, []

].

An analysis was also performed at lower power levels to obtain ROPM as a function of initial power level. The values of CEAW rate, H_{gap} and MTC were chosen based on the parametric analysis performed at 102% power. Hence the [] and []

an MTC of [] $\Delta\rho/^\circ\text{F}$ was used to determine the CEAW rate which allowed []

The results of the CEAW event initiated at 70% and 50% of rated power are given in Figures 6.1-12 and 6.1-13. The maximum ROPM is obtained at 70% and 50% of rated power for reactivity insertion rates of [] $\Delta\rho/\text{inch}$ and [] $\Delta\rho/\text{inch}$, respectively. These CEAW rates in combination with the [] and an MTC of [] $\Delta\rho/^\circ\text{F}$ allow [] by the excore detectors to rise and achieve a new steady state []

The ROPM for the limiting cases initiated at 70% and 50% of rated power are presented in Table 6.1-3.

The ROPM quoted in Table 6.1-3 for the 70% and 50% power cases do not account for any axial shape shift or the decrease in the integrated radial. For the CEAW event initiated at 70% of rated power, the axial shape shift and the decrease in the integrated radial are presented in Figures 6.1-14 and 6.1-15 respectively. The penalty factor that is applied to the ROPM quoted in Table 6.1-3 is given in Figure 6.1-16.

The results indicate that for a CEAW event initiated at axial shape indices [], the margin loss due to axial shape is more than offset by the margin gain due to the decrease in the integrated radial peak. Hence, there is a net margin gain for CEAW event initiated at ASI []].

The penalty factor for an ASI [] is combined with the ROPM quoted in Table 6.1-3 to obtain the final DNB margin degradation at 70% power rated power. Table 6.1-4 and Figure 6.1-17 presents the final ROPM as a function of ASI for the CEAW event initiated at 70% of rated power.

Figures 6.1-18 and 6.1-19 present axial shape shift and the decrease in the F_R as a function of initial AXPD for the CEAW event initiated at 50% power. The penalty factors are presented in Figure 6.1-20. The results show that []

The CEAW event initiated at HZP produces a "spike" in the core heat flux and power. The limiting HZP case is obtained for the combination of [] which produces the maximum rise in core heat flux. This occurs for []. The minimum transient DNBR for the limiting HZP case is 1.4.

The ROPM at the negative extreme of the DNB LCO band allowed at each power level are presented in Figure 6.1-21. The sequence of events for these cases are presented in Tables 6.1-5 to 6.1-8. The responses of key NSSS parameters during a CEAW event are presented in Figure 6.1-23 to 6.1-37. The excore detector responses for the limiting cases at 102%, 70% and 50% of rated power are presented in Figures 6.1-38 to 6.1-40.

The limiting safety analysis cases at all power levels (except HZP) are those where [

] Hence, [

]

6.2 FUEL CENTERLINE TEMPERATURE MELT SAFDL

A parametric analysis in CEAW rate and H_{gap} was performed initiating the transient at 102% of rated power to determine the combination of these parameters which produce the closest approach to fuel centerline melt SAFDL. The results, which are presented in Figure 6.2-1, indicate that the maximum PLHGR is obtained with the [

]. Based on the results at 102% of rated power, []

was used to determine the PLHGR at lower power levels.

The PLHGR as a function of initial power level is presented in Table 6.2-1 and Figure 6.2-2. The transient core power variation at each power analyzed is presented in Figures 6.2-3 to 6.2-6.

As seen from Figure 6.2-2 [

]. Hence, for these power levels, the fuel centerline temperatures (T_Q) are calculated to ensure that UO_2 melt temperatures are not exceeded.

The T_Q calculations are performed for only the HZP case, since the transient initiated at this power results in the longest power spike.

The procedures used to calculate the maximum T_Q are illustrated below for the HZP case. The peak power obtained for the HZP case is 144% of rated thermal power (See Figure 6.2-6) and the power "spike" lasts for 5 seconds. The average energy rise during this time period is equal to []. (The values of $F_{xy}, F_Z, F_A, F_{UNC}$ used to calculate hot spot energy rise are given in Table 4-1). The T_Q rise corresponding to this average energy rise is []. The initial T_Q at HZP is 532°F. Thus, the maximum T_Q is equal to []. This T_Q temperature is below the UO_2 melt temperature of 4800°F at a burnup of 50000 MWD/MT. Hence the fuel centerline melt SAFDL is not exceeded even though the [].

In summary, [

].

TABLE 6.1-1

REQUIRED OVERPOWER MARGIN AT 102% OF RATED POWER

A large, empty rectangular frame with a thin black border, occupying the central portion of the page. It appears to be a placeholder for a table or figure that is not present in this scan.

TABLE 6.1-2

FINAL ROPM AS A FUNCTION OF ASI AT 102% OF RATED THERMAL POWER

Initial ASI	ROPM ₁	Penalty Factor	Final ROPM
-0.14	[]	[]	[]
-0.075	[]	[]	[]
0.0	[]	[]	[]
+0.15	[]	[]	[]
+0.3	[]	[]	[]

TABLE 6.1-3

REQUIRED OVERPOWER MARGIN AT 70% AND 50% OF RATED THERMAL POWER

Initial Power Level (% of 2700 Mwt)	CEAW Rate ($\times 10^{-4} \Delta\rho/\text{inch}$)	MTC ($\times 10^{-4} \Delta\rho/^\circ\text{F}$)	H_{gap}^2 BTU/hr-ft ² -°F	ROPM
70	[]	[]	[]	[]
50	[]	[]	[]	[]

TABLE 6.1-4

FINAL ROPM AS A FUNCTION OF ASI AT 70% OF RATED THERMAL POWER

Initial ASI	ROPM ₁	Penalty Factor	Final ROPM
-0.4	[]	[]	[]
-0.15	[]	[]	[]
0	[]	[]	[]
+0.15	[]	[]	[]
+0.3	[]	[]	[]

TABLE 6.1-5

Sequence of Events for
CEA Withdrawal Event Initiated at
102% of Rated Power

<u>Time (Sec)</u>	<u>Event</u>	<u>Value</u>
0.0	CEAs begin to Withdraw	
68.5	CEAs Completely Withdrawn	
220	[]	[]
220	[]	[]
300	[]	[]
300	[]	[]
482	[]	[]

TABLE 6.1-6

Sequence of Events for
CEA Withdrawal Event Initiated at
70% of Rated Power

<u>Time (Sec)</u>	<u>Event</u>	<u>Value</u>
0.0	CEAs begin to Withdraw	
164.4	CEAs Completely Withdrawn	
250.0	[]	[]
250.0	[]	[]
310.	[]	[]
310	[]	[]
550.0	[]	[]

TABLE 6.1.7

Sequence of Events for
CEA Withdrawal Event Initiated at
50% of Rated Power

<u>Time (Sec)</u>	<u>Event</u>	<u>Value</u>
0.0	CEAs begin to Withdraw	-
342.5	CEAs Completely Withdrawn	-
400	[]	[]
400	[]	[]
429.0	[]	[]
429:0	[]	[]
600.0	[]	[]

TABLE 6.1-8

Sequence of Events for
CEA Withdrawal Event Initiated at HZP

<u>Time (Sec)</u>	<u>Event</u>	<u>Value</u>
0.0	CEAs begin to Withdraw	
34.1	Reactor Trip on High Power, % of 2710 MWt	40
34.5	Trip Breakers Open	--
34.9	Shutdown CEA's begin to Drop into Core	--
35.2	Maximum Core Power, % of 2710 MWt	144
36.5	Maximum Core Heat Flux, % of 2710 MWt	68.4
38.6	Maximum RCS Pressure, psia	2366

TABLE 6.2-1

PLHGR AS A FUNCTION OF POWER LEVEL

Initial Power Level (% of 2710 MWt)	CEAW Rate $\times 10^{-4} \Delta\rho/\text{inch}$	H_{gap} BTU/hr-ft ² -°F	Initial LHGR (KW/FT)	ΔPLHGR	PLHGR (KW/FT)
102	[]	[]	[]	[]	[]
70	[]	[]	[]	[]	[]
50	[]	[]	[]	[]	[]
HZP	[]	[]	[]	[]	[]

CEA WITHDRAWAL EVENT FROM 102% POWER
ROPM (DMR) vs CEA REACTIVITY
INSERTION RATE

Figure
6.1-1

CEA WITHDRAWAL EVENT FROM 102% POWER
ROPM (D/D) vs CEA REACTIVITY
INSERTION RATE

Figure
6.1-2

CEA WITHDRAWAL EVENT FROM 102% POWER
ROPM (NDR) vs CEA REACTIVITY
INSERTION RATE

FIGURE
6.1-3

CLA WITHDRAWAL EVENT FROM 100% POWER
ROPAL (DMSR) vs CLA REACTIVITY
INSERTION RATE

Figure
6.1-4

CEA WITHDRAWAL EVENT FROM 102% POWER
REQUIRED OVERPOWER MARGIN vs CEA
WITHDRAWAL RATE

Figure
6.1-5

CEA WITHDRAWAL EVENT FROM 102% POWER
REQUIRED OVERPOWER MARGIN vs CEA
WITHDRAWAL RATE

Figure
6.1-6

CEA WITHDRAWAL EVENT FROM 102% POWER
REQUIRED OVERPOWER MARGIN (DNBR) vs CEA
REACTIVITY INSERTION RATE

Figure
6.1-7

CEA WITHDRAWAL EVENT FROM 102% POWER
AXIAL SHAPE INDEX SHIFT vs INITIAL AXIAL
SHAPE INDEX

Figure
6.1-8

CEA WITHDRAWAL EVENT FROM 102% POWER
INTEGRATED RADIAL DECREASE vs INITIAL
AXIAL SHAPE INDEX

Figure
6.1-9

CEA WITHDRAWAL EVENT FROM 102% POWER
PENALTY FACTOR ON DNB ROPM vs INITIAL
AXIAL SHAPE INDEX

Figure
6.1-10

CEA WITHDRAWAL EVENT FROM 102% POWER
ROPM (DNB) vs INITIAL AXIAL SHAPE INDEX

Figure
6.1-11

CEA WITHDRAWAL EVENT FROM 70% POWER
REQUIRED OVERPOWER MARGIN vs CEA
WITHDRAWAL RATE

Figure
6.1-12

CEA WITHDRAWAL EVENT FROM 50% POWER
REQUIRED OVERPOWER MARGIN vs CEA
WITHDRAWAL RATE

Figure
6.1-13

CEA WITHDRAWAL EVENT FROM 70% POWER
AXIAL SHAPE INDEX SHIFT vs INITIAL AXIAL
SHAPE INDEX

Figure

6.1-14

CEA WITHDRAWAL EVENT FROM 70% POWER
INTEGRATED RADIAL DECREASE vs INITIAL AXIAL
SHAPE INDEX

Figure
6.1-15

CEA WITHDRAWAL EVENT FROM 70% POWER
PENALTY FACTOR ON DNB ROPM vs INITIAL
AXIAL SHAPE INDEX

Figure
6.1-16

CEA WITHDRAWAL EVENT FROM 70% POWER
ROPM (DNBR) vs INITIAL AXIAL SHAPE INDEX

Figure
6.1-17

CEA WITHDRAWAL EVENT FROM 50% POWER
AXIAL SHAPE SHIFT vs INITIAL AXIAL
SHAPE INDEX

Figure
E.1-18

CEA WITHDRAWAL EVENT FROM 50% POWER
INTEGRATED RADIAL DECREASE vs INITIAL AXIAL
SHAPE INDEX

Figure
6.1-19

CEA WITHDRAWAL EVENT FROM 50% POWER
PENALTY FACTOR ON DNB ROMM vs INITIAL
AXIAL SHAPE INDEX

Figure

6.1-20

CEA WITHDRAWAL EVENT
REQUIRED OVERPOWER MARGIN
VS INITIAL POWER

Figure

6.1-21

CEA WITHDRAWAL EVENT FROM 102% POWER
CORE POWER vs TIME

FIGURE

6.1-22

CEA WITHDRAWAL EVENT FROM 102% POWER
CORE AVERAGE HEAT FLUX vs TIME

FIGURE
6.1-23

CEA WITHDRAWAL EVENT FROM 102% POWER
RCS TEMPERATURES vs TIME

FIGURE
6.1-24

CEA WITHDRAWAL EVENT FROM 102% POWER
RCS PRESSURE vs TIME

Figure
E.1-25

CEA WITHDRAWAL EVENT AT 70% POWER
CORE POWER vs TIME

FIGURE

5.1-25

CEA WITHDRAWAL EVENT FROM 70% POWER
CORE AVERAGE HEAT FLUX vs TIME

FIGURE
6.1-27

CEA WITHDRAWAL EVENT FROM 70% POWER
RCS TEMPERATURE vs TIME

FIGURE
E.1-28

CEA WITHDRAWAL EVENT FROM 70% POWER
RCS PRESSURE vs TIME

Figure
6.1-29

CEA WITHDRAWAL EVENT FROM 50% POWER
CORE POWER vs TIME

FIGURE
6.1-30

CEA WITHDRAWAL EVENT FROM 50% POWER
CORE AVERAGE HEAT FLUX vs TIME

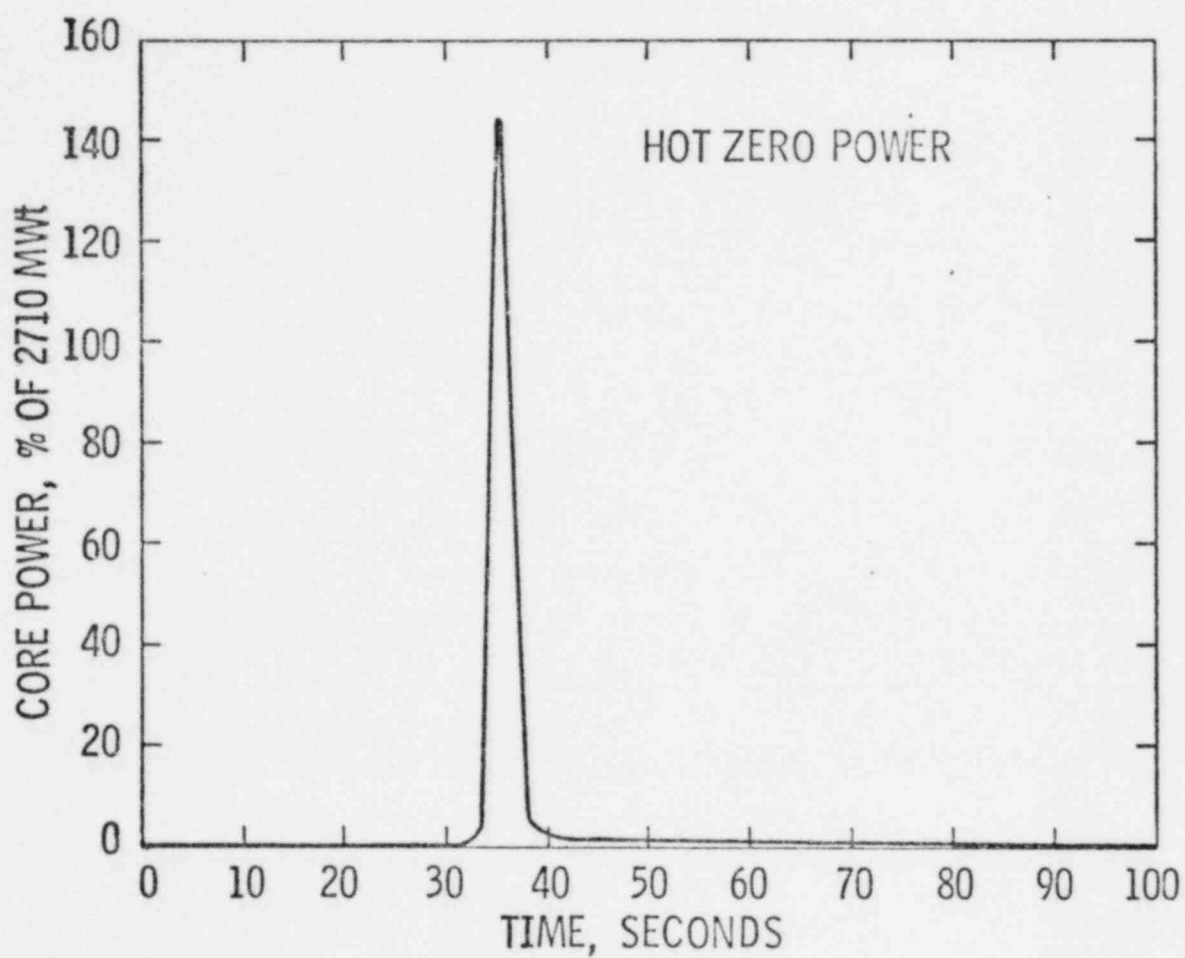
FIGURE
6.1-31

CEA WITHDRAWAL EVENT FROM 50% POWER
RCS TEMPERATURE vs TIME

FIGURE
6.1-32

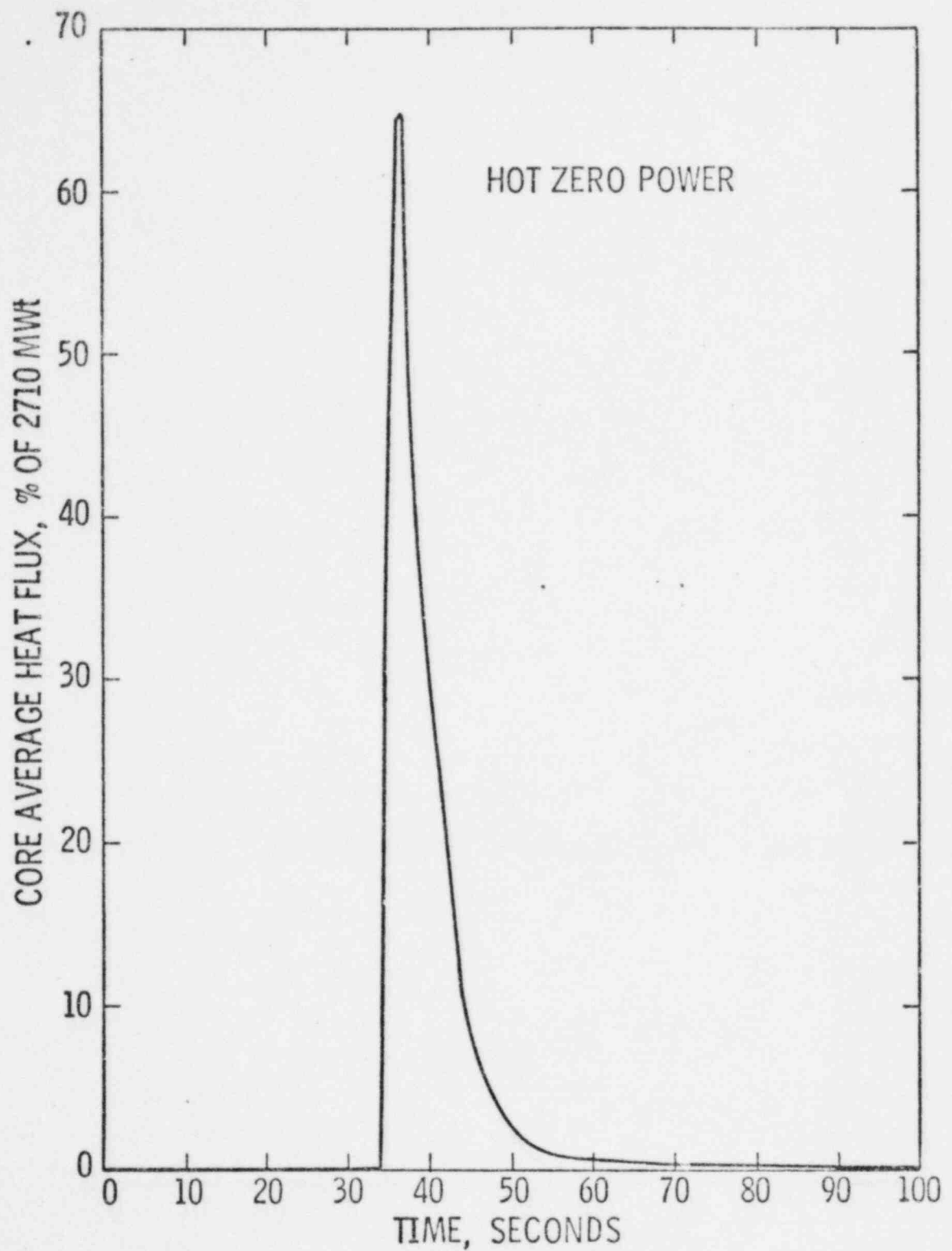
CEA WITHDRAWAL EVENT FROM 50% POWER
RCS PRESSURE vs TIME

Figure
6.1-33



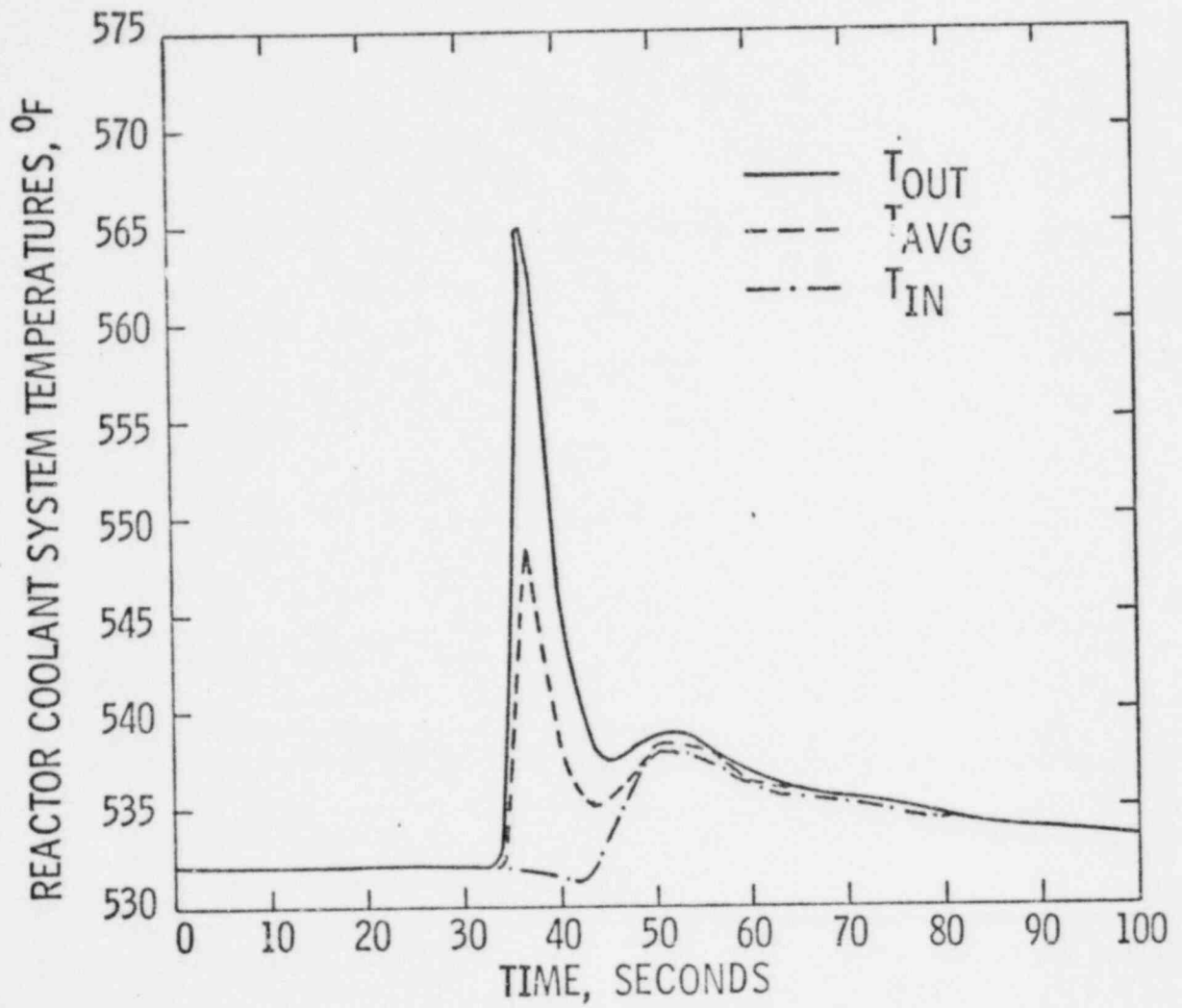
CEA GROUP WITHDRAWAL EVENT
CORE POWER vs TIME

FIGURE
6.1-34



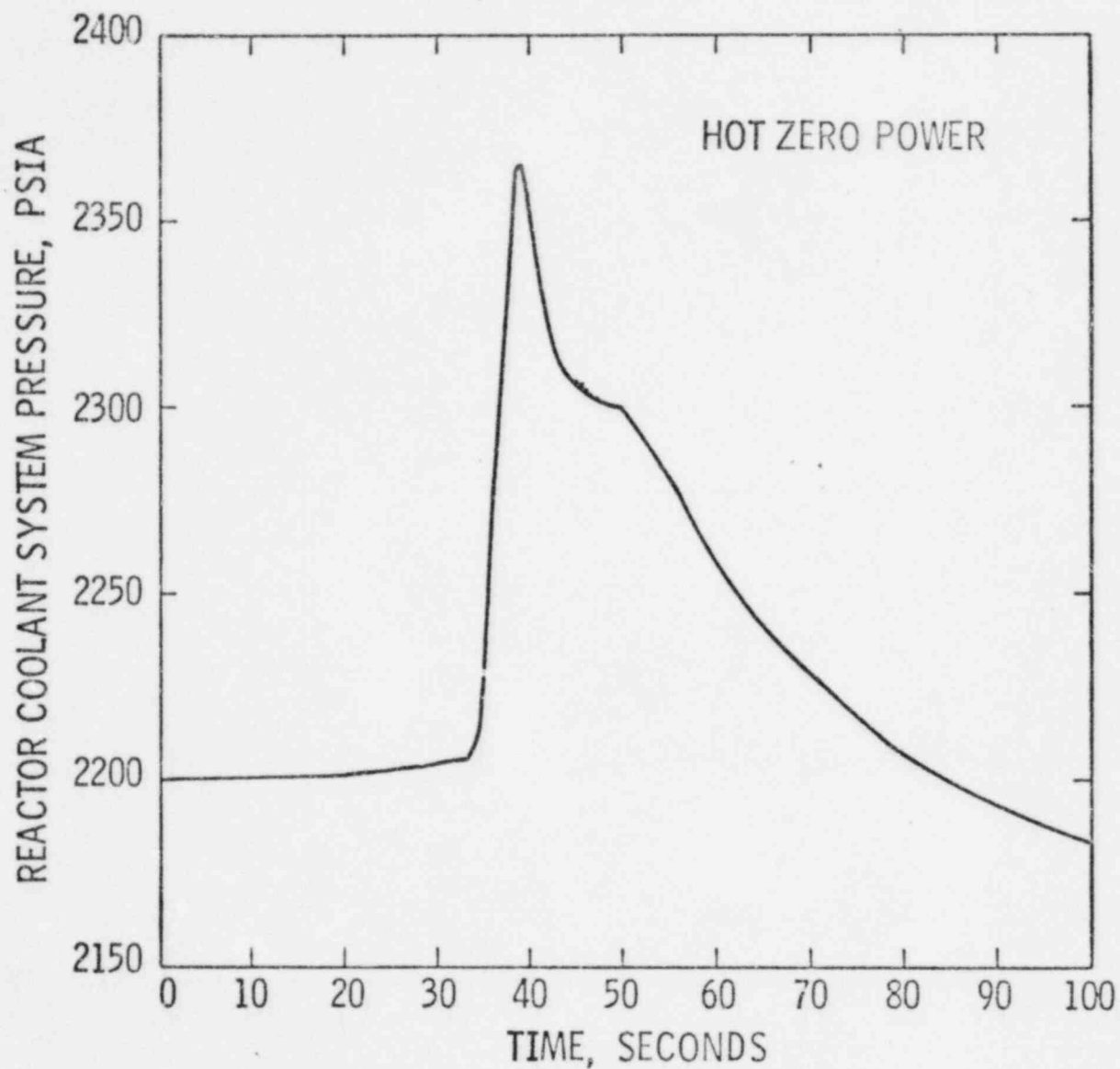
CEA GROUP WITHDRAWAL EVENT
CORE AVERAGE HEAT FLUX vs TIME

FIGURE
6.1-35



CEA WITHDRAWAL EVENT FROM HZP
RCS TEMPERATURE vs TIME

FIGURE
6.1-36



CEA GROUP WITHDRAWAL EVENT
REACTOR COOLANT SYSTEM PRESSURE vs TIME

FIGURE
6 7

CEA WITHDRAWAL EVENT FROM 102% POWER
EXCORE DETECTOR POWER MEASUREMENT vs TIME

FIGURE
6.1-38

CEA WITHDRAWAL EVENT FROM 70% POWER
EXCORE DETECTOR POWER MEASUREMENT vs TIME

FIGURE
6.1-39

CEA WITHDRAWAL EVENT FROM 50% POWER
EXCORE DETECTOR POWER MEASUREMENT vs TIME

FIGURE
6.1-40

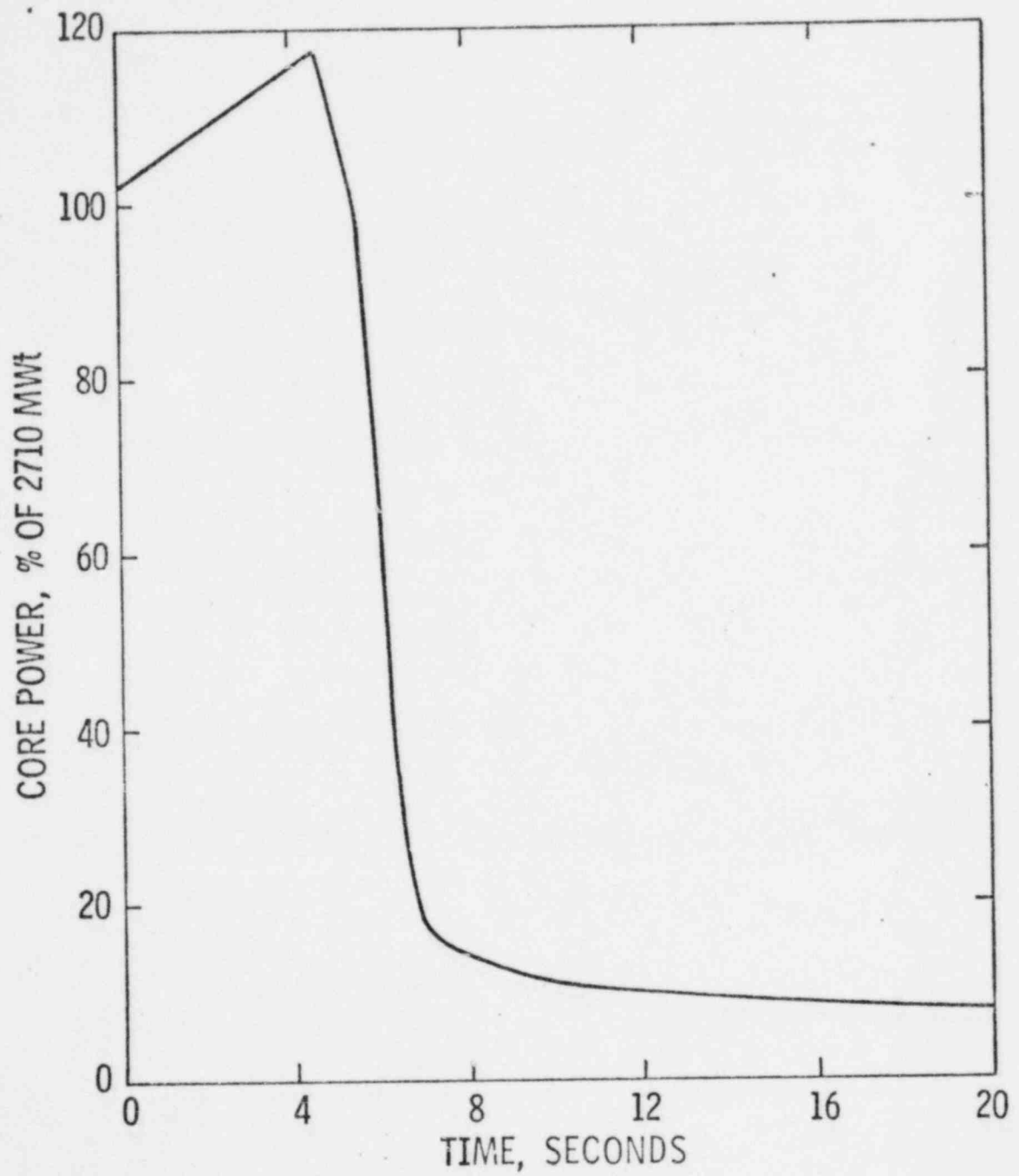
CEA GROUP WITHDRAWAL EVENT
PEAK LINEAR HEAT GENERATION RATE vs Hgap

FIGURE

6.2-1

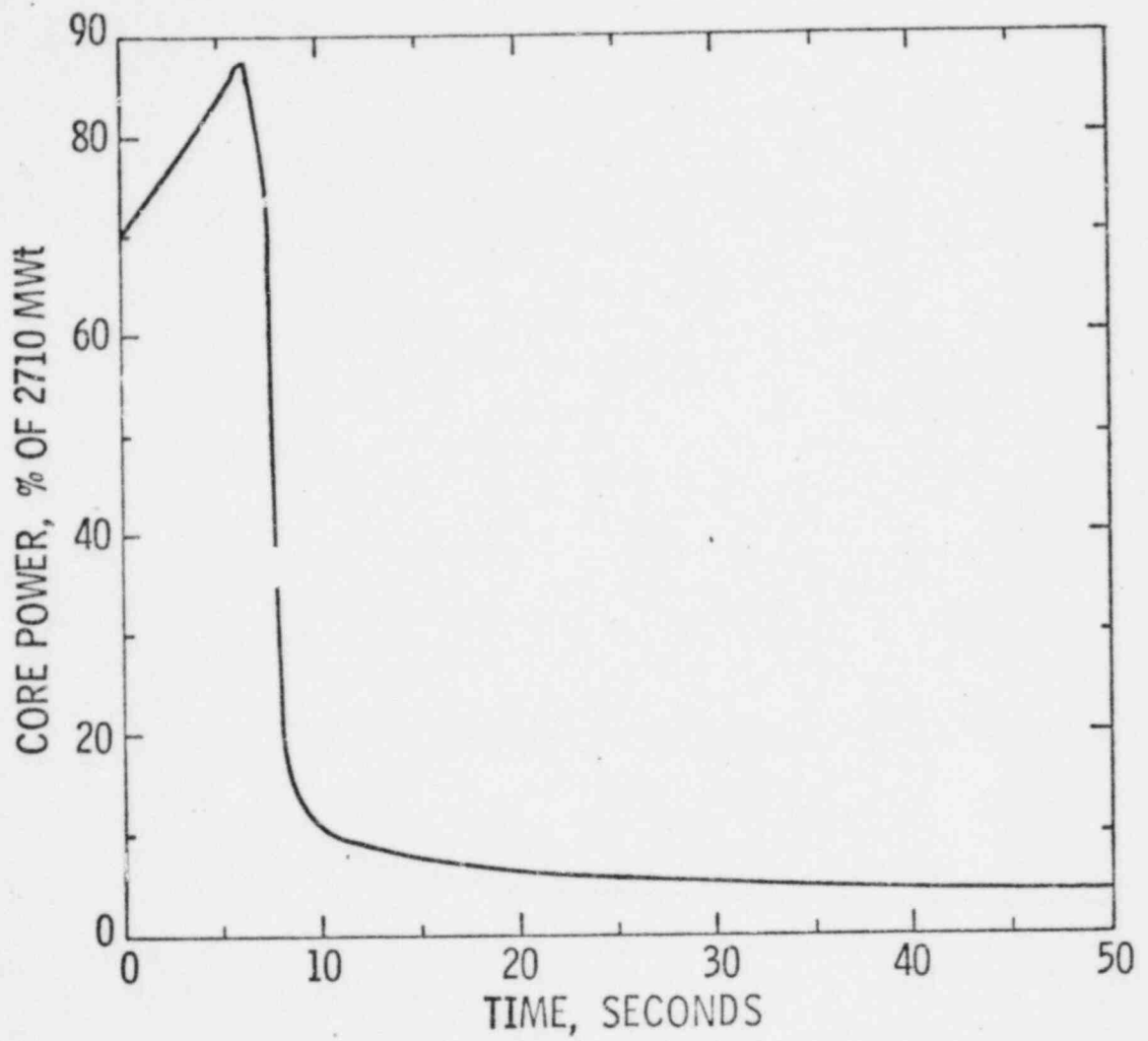
CEA GROUP WITHDRAWAL EVENT
PEAK LINEAR HEAT GENERATION RATE vs INITIAL POWER

FIGURE
E.2-2



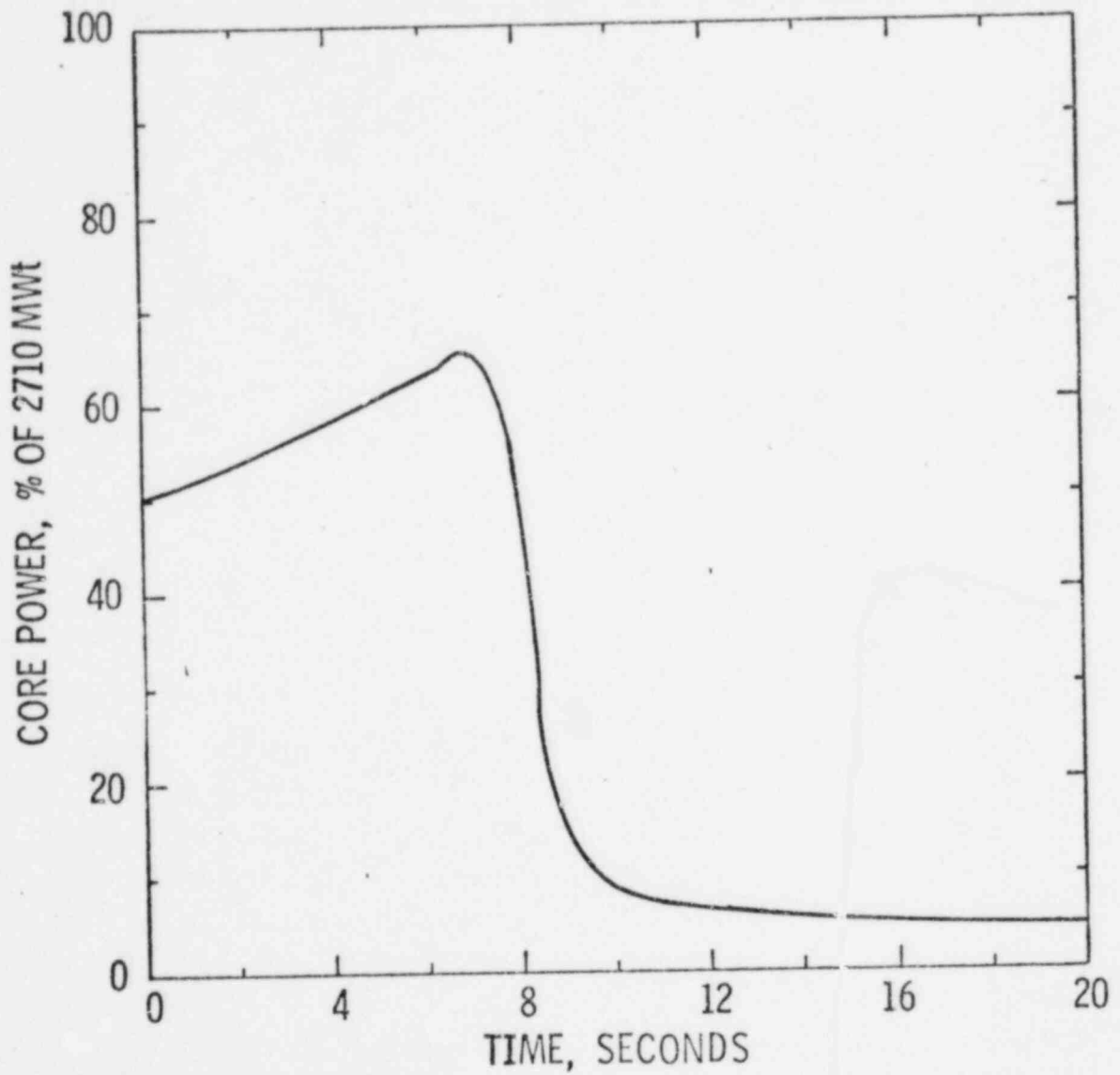
CEA WITHDRAWAL EVENT FROM 102% POWER
CORE POWER vs TIME

FIGURE
6.2-3



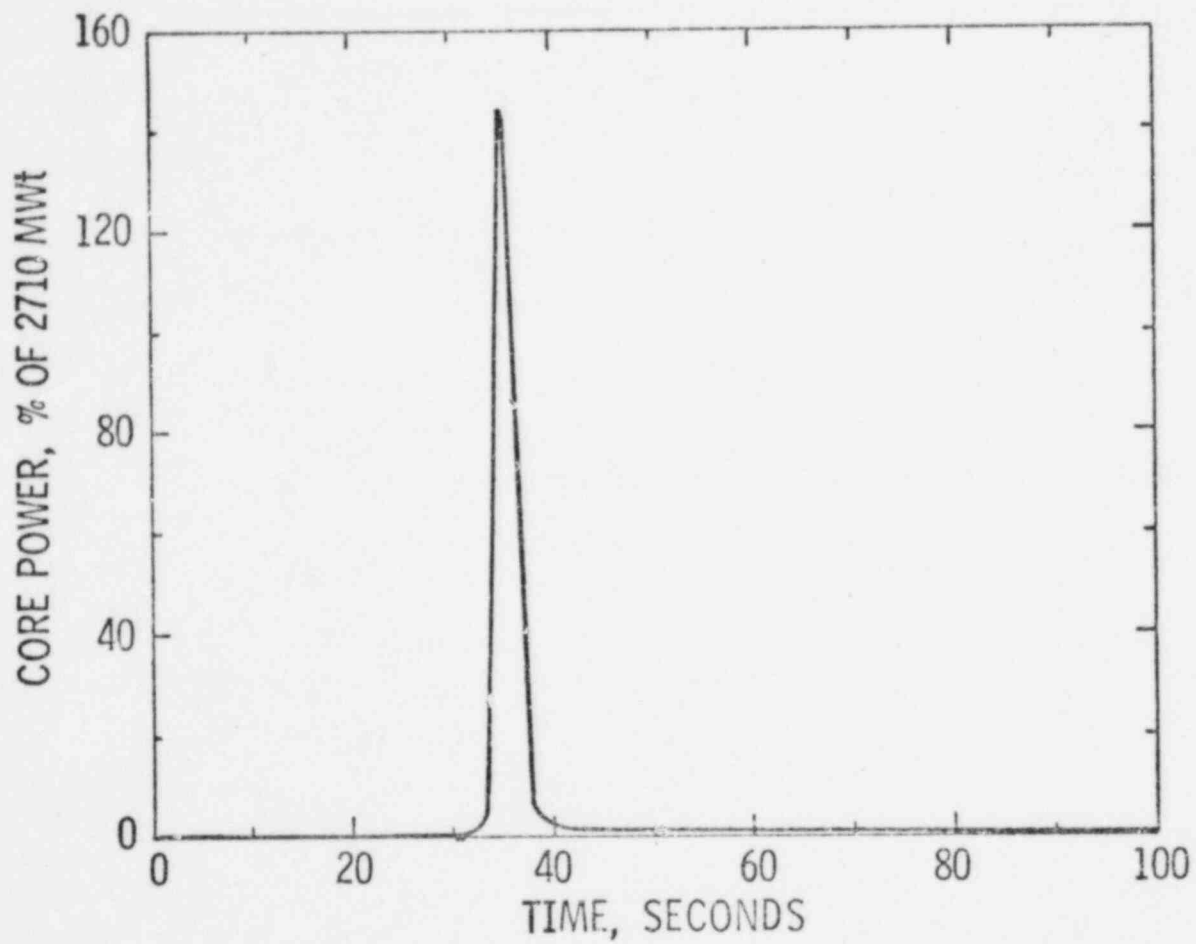
CEA WITHDRAWAL EVENT FROM 70% POWER
CORE POWER vs TIME

FIGURE
6.2-4



CEA WITHDRAWAL EVENT FROM 50% POWER
CORE POWER vs TIME

FIGURE
6.2-5



CEA WITHDRAWAL EVENT FROM HZP
CORE POWER vs TIME

FIGURE
6.2-6

7. CONSERVATISMS IN ANALYTICAL METHODS

The purpose of this section is to identify the conservatisms that are included in the methods used to calculate the ROPM on DNBK and peak linear heat generation rate. (These conservatisms are qualitatively identified below). Example cases are presented and compared with the safety analysis results of previous sections to quantify the conservatisms.

1. The power input to the high power trip (HPT) and the variable high power trip (VHPT) is the auctioneered higher of the neutron flux power (measured by excore detectors) and the thermal power (measured by the ΔT -Power Calculator). [

]. The analysis assumed a reactor trip is initiated on the HPT or the VHPT [

].

2. The CEAW event initiated at 102% of rated power assumed a HPT setpoint of 112% of initial power. This includes a transient decalibration uncertainty of 3%. The transient decalibration of the excore detectors which is explicitly accounted for in the safety analysis is less than 3%.
3. The MTC is not expected to be positive except for the first few hundred MWD/MT. This occurs only at zero power.
4. The k_{gap} value is higher than expected on a core average basis at the end of a given reload cycle.

5. The calculation of PLHGR used the maximum value for CEA reactivity insertion rate. This maximum value is higher than expected for any reload cycle.
6. In computing margin requirements, [

].

7.1 CONSERVATISMS IN DNB ROPM CALCULATIONS

To quantify the conservatisms outlined above, two "best estimate" cases were run. The first, initiated at 100% of rated power and the second initiated at 50% of rated power. A comparison of the input data used in the safety analysis cases described in Sections 5 and 6 with that used in the best estimate cases are presented in Table 7.1-1 and 7.1-2.

The sequence of events for the best estimate cases are presented in Tables 7.1-3 and 7.1-4. A comparison of the ROPM's for the best estimate case and the safety analysis cases are presented below.

<u>Initial Power Level (% of 2710 MWt)</u>	<u>ROPM (% of Initial Power)</u>	
	Best Estimate	Safety Analysis
102	[]	[]
50	[]	[]

The above comparison shows that the safety analysis ROPM's are at least [] conservative with respect to the best estimate results. The results of best estimate analysis at 102% of rated power shows that the power and heat flux rise but the increasing coolant temperatures in combination with the

negative MTC adds negative reactivity which reduces the power and heat flux to their initial values and achieve a steady state condition. The response of the NSSS for the best estimate cases are presented in Figure 7.1-1 to 7.1-8.

7.2 CONSERVATISMS IN PEAK LINEAR HEAT GENERATION RATE

The conservatisms in the PLHGR calculations were quantified by performing best estimate cases. The first, performed at 102% of rated power and second performed at HZP.

The transient core power rises for the best estimate cases are presented in Figures 7.2-1 and 7.2.2. A comparison of best estimate and safety analysis results are presented below.

Initial Power % of 2710 MWt	SAFETY ANALYSIS		BEST ESTIMATE ANALYSIS	
	Δ PLHGR	PLHGR	Δ PLHGR	PLHGR
102	[]	[]	[]	[]
HZP	[]	[]	[]	[]

The results show that at full power the PLHGR is conservative by [] This due to the conservative value of CEAW rate assumed in the safety analysis to bound all future reload cycles. The results also show that the steady state limit of 21KW/ft is exceeded for the best estimate case. This is to be expected since at HZP, the transient produces a power spike. A calculation was performed to determine the T_c and results are given below.

	Average ΔE rise (BTU/lbm)	Hot Spot ΔE rise (BTU/lbm)	ΔT rise $^{\circ}F$	T_{GL} initial $^{\circ}F$	T_{GL} max $^{\circ}F$
Safety Analysis	[]	[]	[]	532	[]
Best Estimate Analysis	[]	[]	[]	532	[]

The results show that the T_{GL} calculated is conservative by at least []. Hence based on this comparison we can conclude that the results presented in Section 5.2 are sufficiently conservative.

TABLE 7.1-1

KEY INPUT PARAMETERS USED IN CEAW EVENT ANALYSIS INITIATED FROM 102% POWER

<u>Parameters</u>	<u>Units</u>	<u>Safety Analysis Values</u>	<u>Safety Analysis Values with Identified Conservatism Eliminated</u>
Initial Power Level	% of 2710 MWt	102	<u>< 102</u> **
Initial Inlet Temperature	°F	550	<u>< 550</u> **
Initial RCS Pressure	psia	2200	<u>>2200</u> **
Initial Core Flow	$\times 10^6$ lbm/hr-ft ²	2.53	<u>>2.53</u> **
Moderator Temperature Coefficient	$\times 10^{-4}$ $\Delta\rho$ /°F	[]	[]
Gap Thermal Conductivity	BTU/hr-ft ² -°F	[]	[]
CEA Differential Worth	10^{-4} $\Delta\rho$ /inch	[]	[]
CEA Withdrawal Speed	inch/minute	30	30
CEA Worth at Trip	% $\Delta\rho$	-4.6	<u>> -5.8</u> **
High Power Trip Setpoint	% of 2710 MWt	112.0	109.0
Integrated Radial, F_R		1.65	1.65
Temperature Shadowing Factor	% power/°F	[]	[]
ΔT -Power Setpoint Coefficients (a, τ)		*	(2.5, .1)
Axial Shape Index		[]	[]

* NOT TAKEN CREDIT FOR IN SAFETY ANALYSIS

** Results insensitive to initial values for these parameters.

TABLE 7.1-2

KEY INPUT PARAMETERS USED IN CEAW EVENT ANALYSIS INITIATED FROM 50% POWER

<u>Parameters</u>	<u>Units</u>	<u>Safety Analysis Values</u>	<u>Safety Analysis Values With Identified Conservatisms Eliminated</u>
Initial Power Level	% of 2710 Mwt	50	50
Initial Inlet Temperature	°F	540	≤ 540**
Initial RCS Pressure	psia	2200	≥ 2200**
Initial Core Flow	$\times 10^6$ lbm/hr-ft ²	2.53	≥ 2.53**
Moderator Temperature Coefficient	$\times 10^{-4}$ Δρ/°F	[]	[]
Gap Thermal Conductivity	BTU/hr-ft ² -°F	[]	[]
CEA Differential Worth	10^{-4} Δρ/inch	[]	[]
CEA Withdrawal Speed	inch/minute	30	30
CEA Worth at Trip	% Δρ	-3.4	≥ -4.3
High Power Trip Setpoint	% of 2710 Mwt	60	60
Integrated Radial, F _R		2.0	≤ 2.0 **
Temperature Shadowing Factor	% power/°F	[]	[]
ΔT-Power Setpoint Coefficients (a, τ)		*	(2.5, .1)
Axial Shape Index		[]	[]

*Not taken credit for in safety analysis.

** Results insensitive to initial values for these parameters.

TABLE 7.1-3

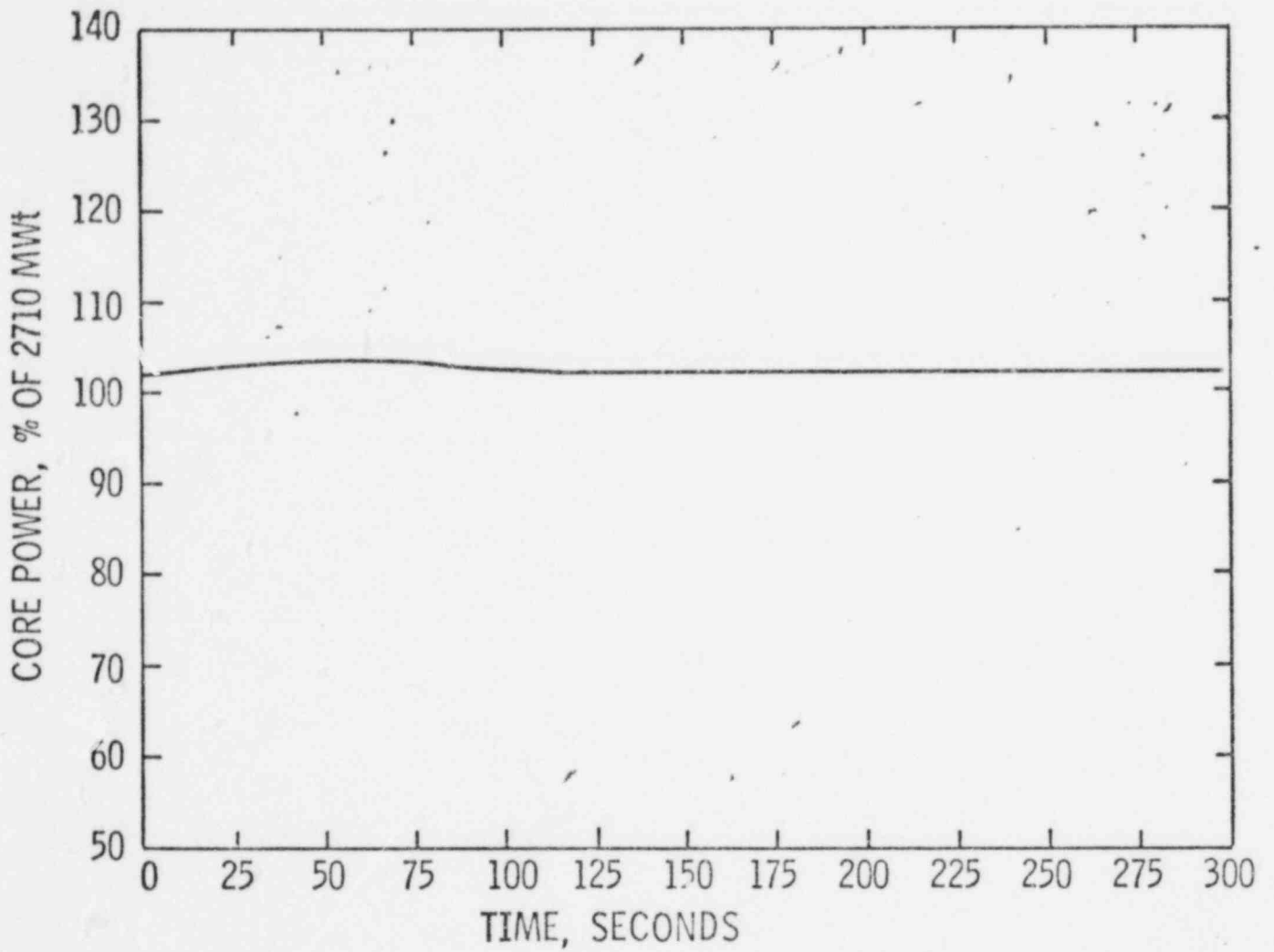
SEQUENCE OF EVENTS FOR
CEA WITHDRAWAL EVENT INITIATED AT 102% OF
RATED POWER
(Best estimate)

<u>TIME</u>	<u>EVENT</u>	<u>VALUE</u>
0.0	CEA's Begin to Withdraw	-
68.5	CEA's Completely Withdrawn	-
69.5	Maximum Power, % of 2710 MWt	103.5
73.0	Maximum Heat Flux, % of 2710 MWt	103.4
125.0	Maximum Inlet Temperature, °F	552.7
128.0	Maximum RCS Pressure, psia	2274
158.0	Core Power Returns to it's Initial Value, % of 2710 MWt	102
166.0	Core Heat Flux Returns to it's Initial Value, % of 2710 MWt	102

TABLE 7.1-4

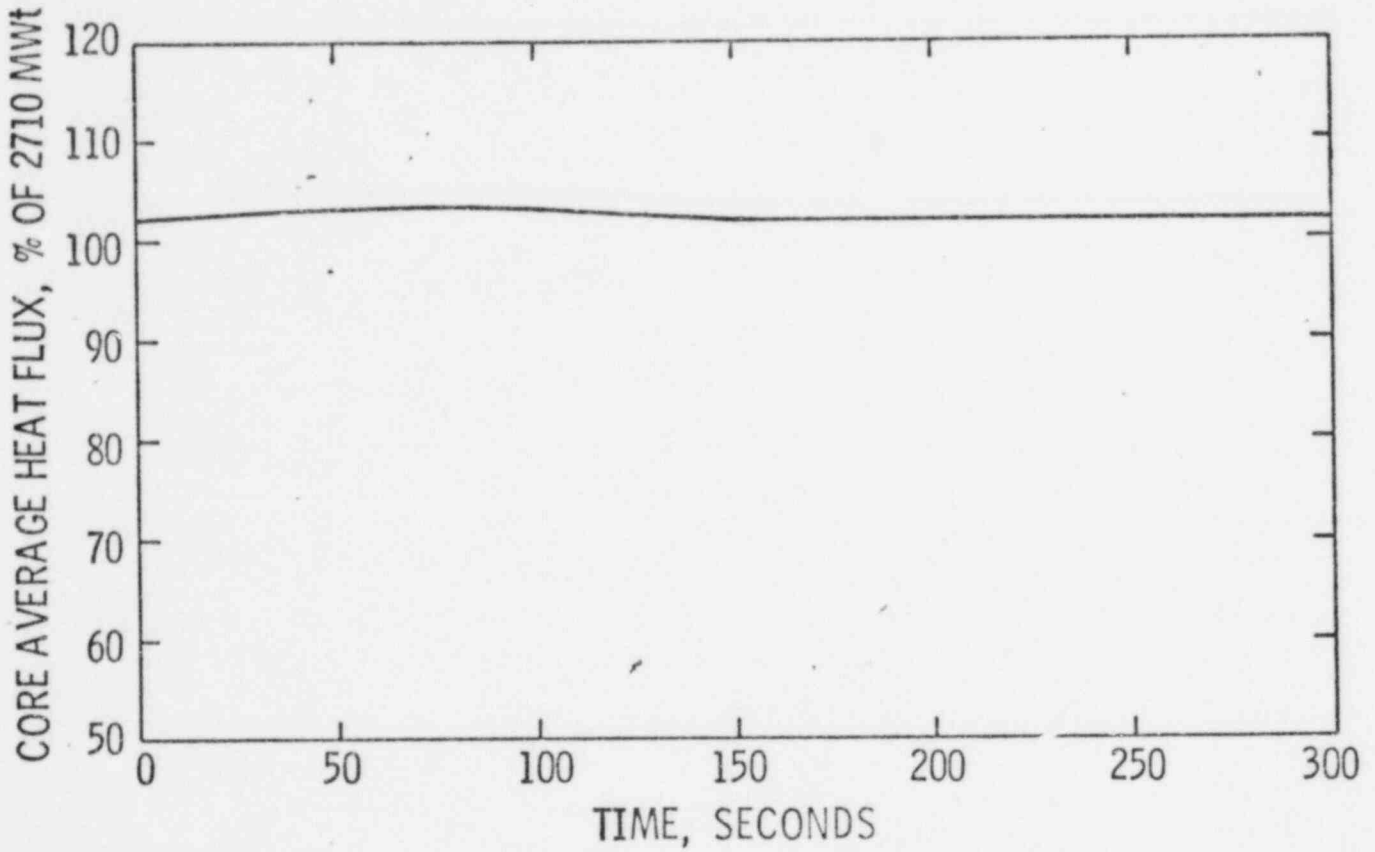
SEQUENCE OF EVENTS FOR
CEA WITHDRAWAL EVENT INITIATED AT 50% OF
RATED POWER
(Best estimate)

<u>TIME</u>	<u>EVENT</u>	<u>VALUE</u>
0.0	CEA's Begin to Withdraw	
55.0.	Reactor Trip on High Power	60%
55.4	Trip Breakers Open	
55.9	Shutdown CEA's Begin to Drop into Core	
56.2	Maximum Power, % of 2710 MWt	62.0
56.7	Maximum Heat Flux, % of 2710 MWt	61.3
57.4	Maximum RCS Pressure, psia	2353
70.5	Maximum Inlet Temperature, °F	548.2

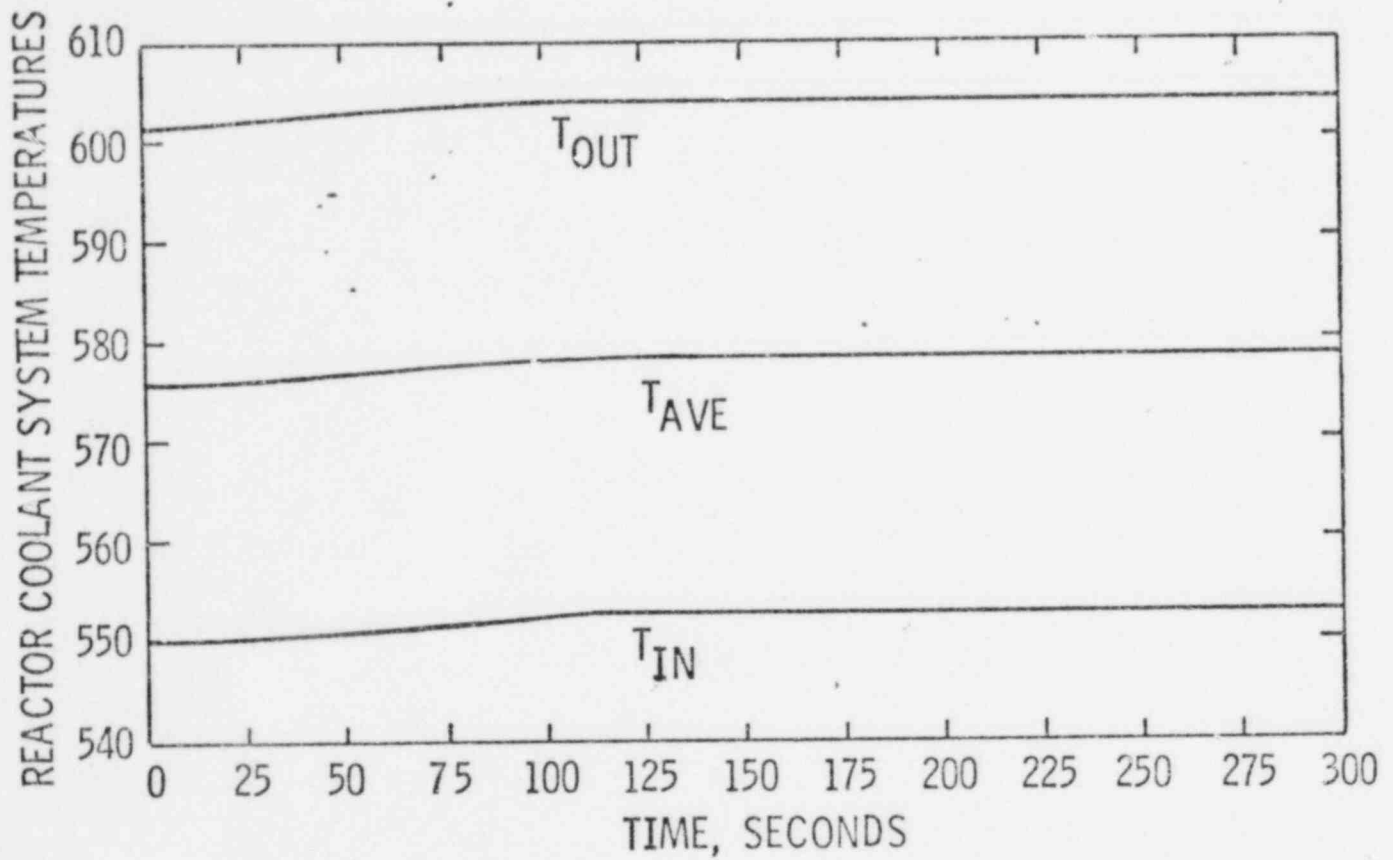


CEA WITHDRAWAL EVENT FROM 102% POWER
CORE POWER vs TIME

Figure
7.1-1

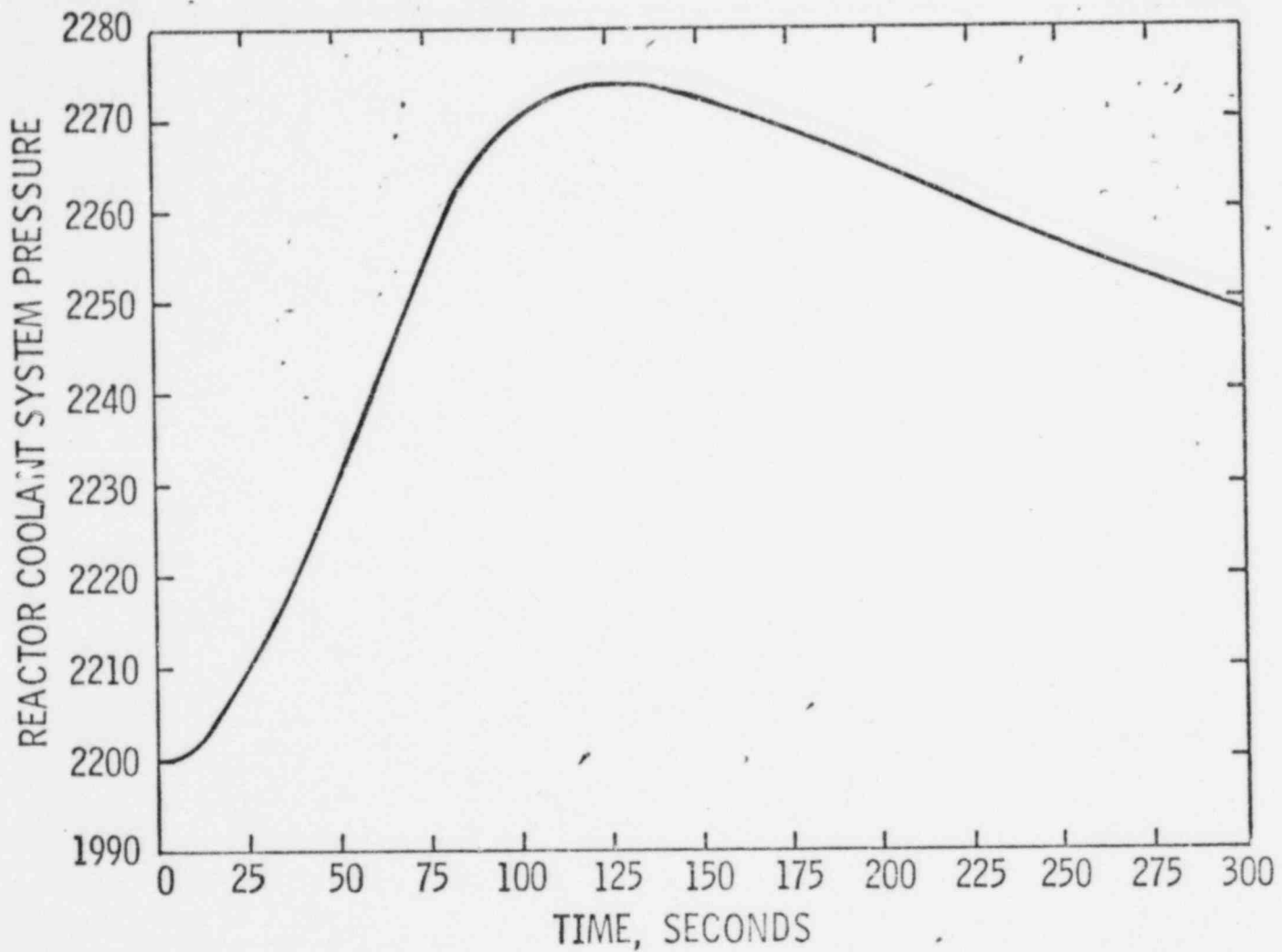


	CEA WITHDRAWAL EVENT FROM 102% POWER CORE AVERAGE HEAT FLUX vs TIME	Figure 7.1-2
--	--	-----------------



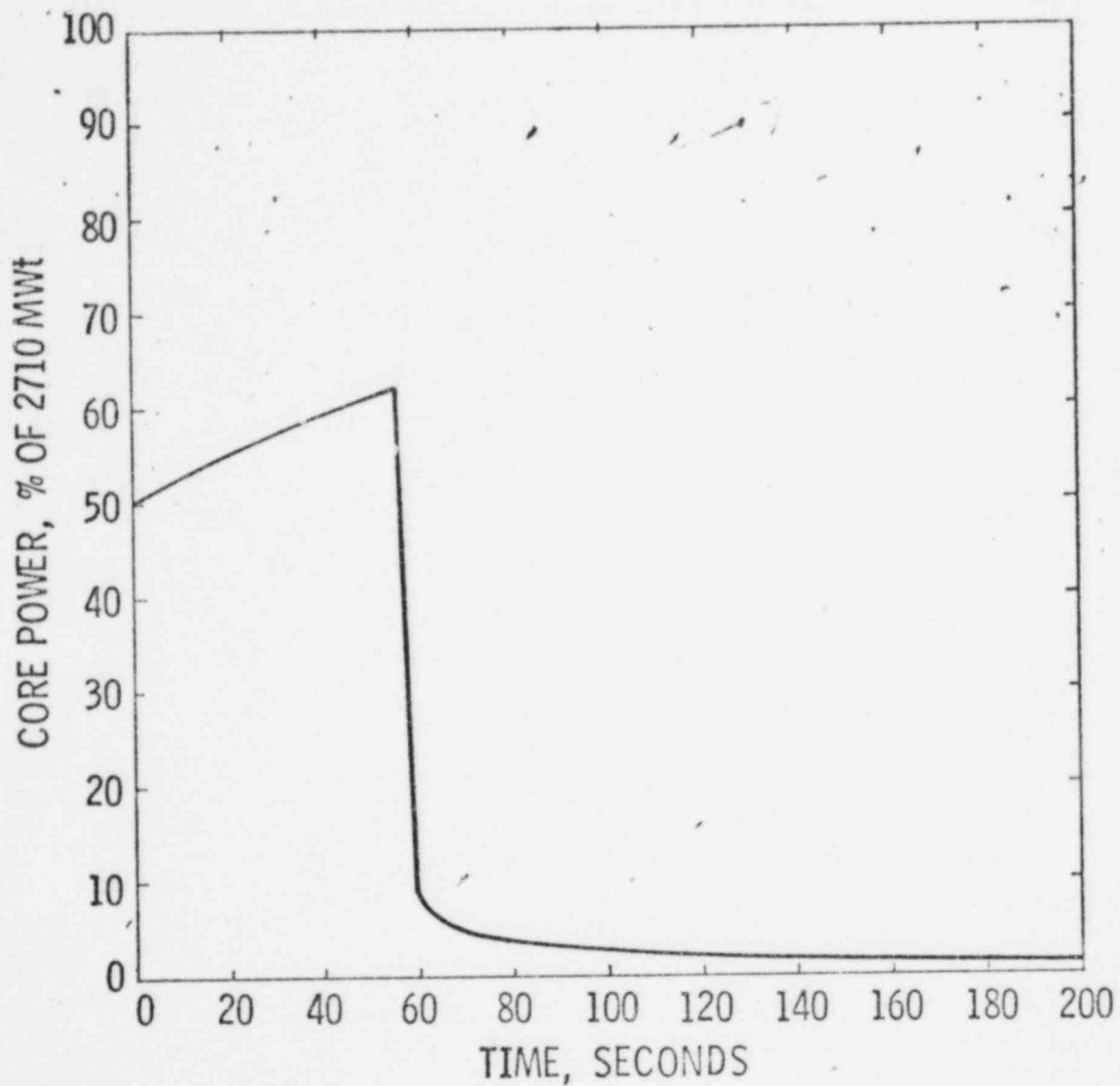
CEA WITHDRAWAL EVENT FROM 102% POWER
RCS TEMPERATURE vs TIME

Figure
7.1-3



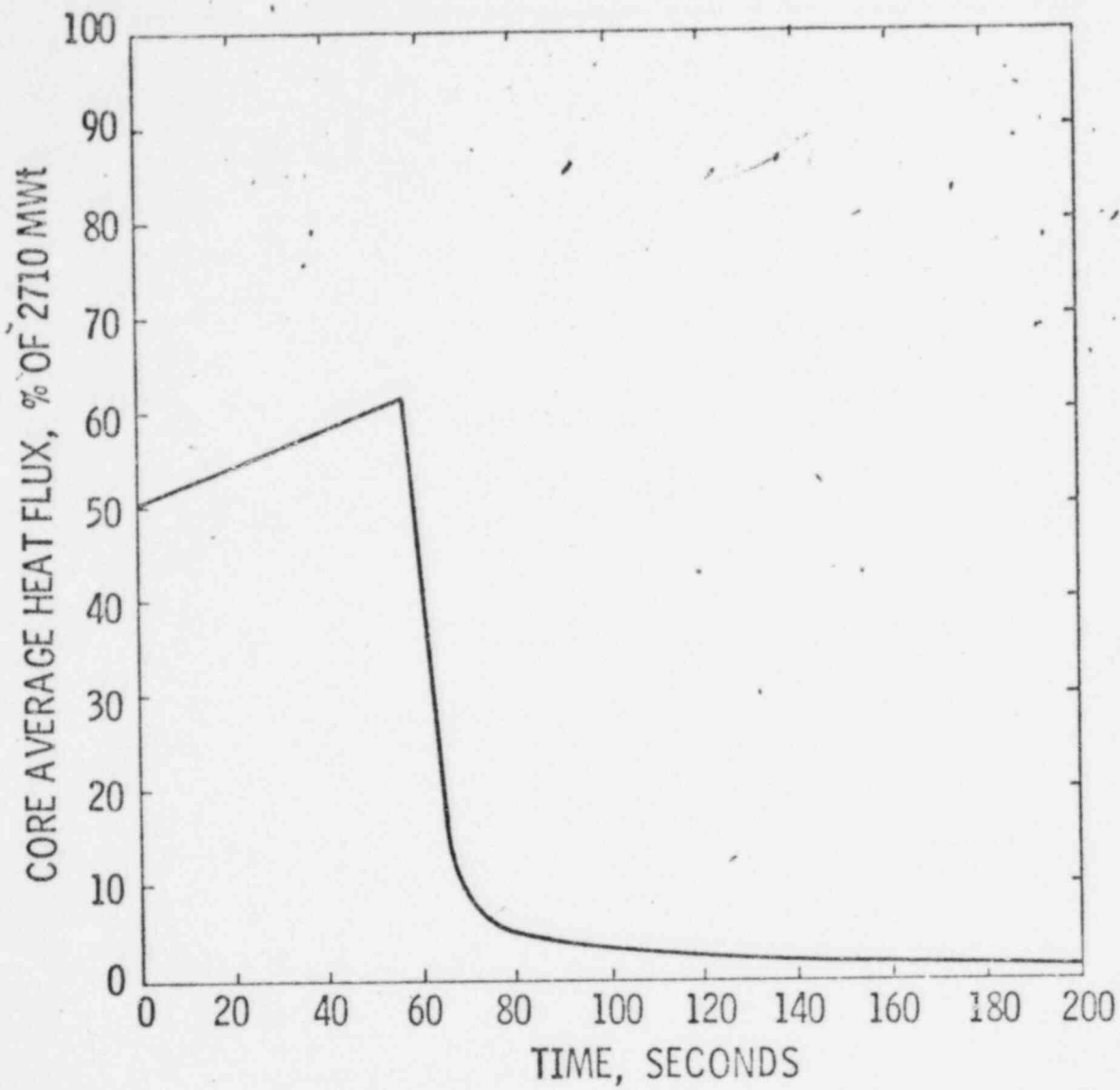
CEA WITHDRAWAL EVENT FROM 102% POWER
RCS PRESSURE vs TIME

Figure
7.1-4

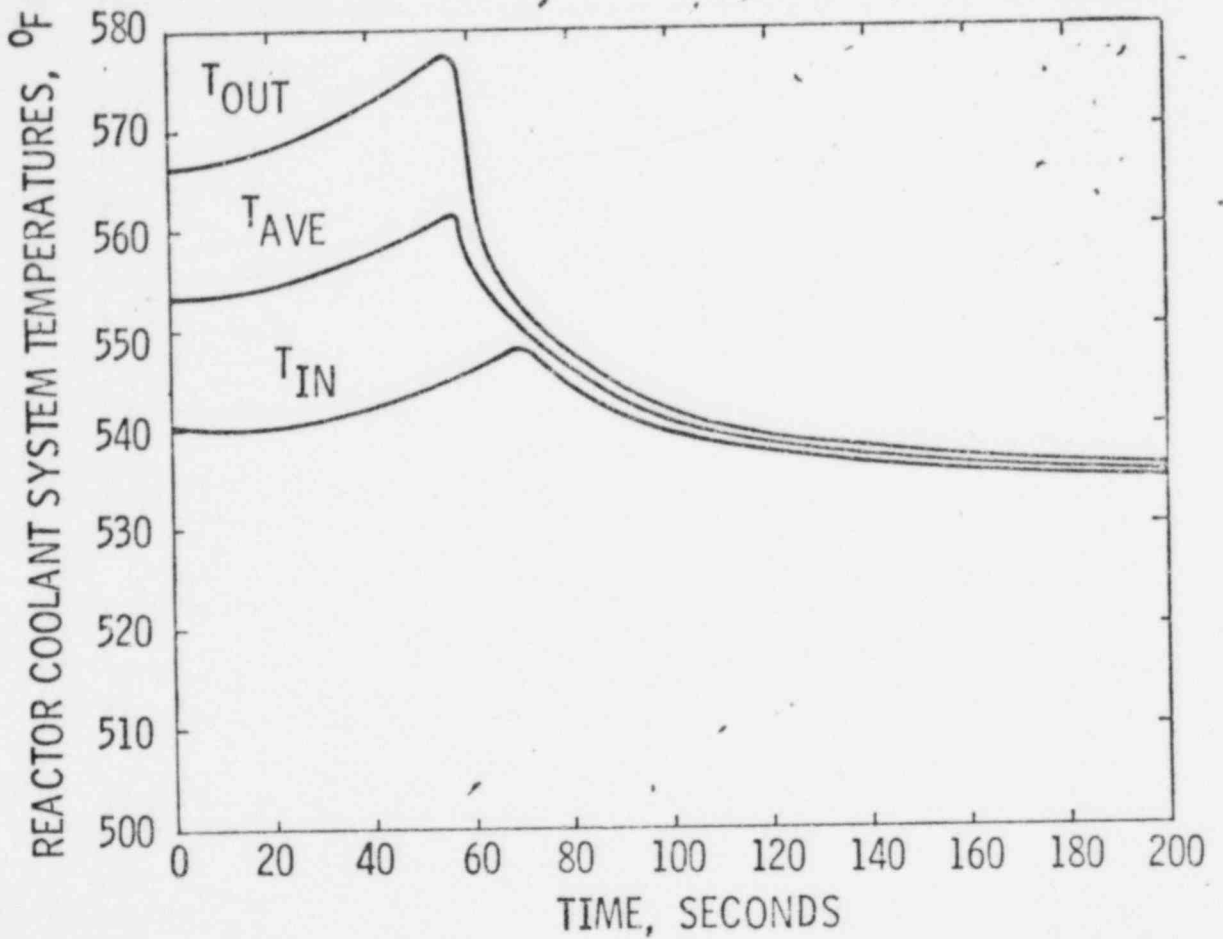


CEA WITHDRAWAL EVENT FROM 50% POWER
CORE POWER vs TIME

Figure
7.1-5

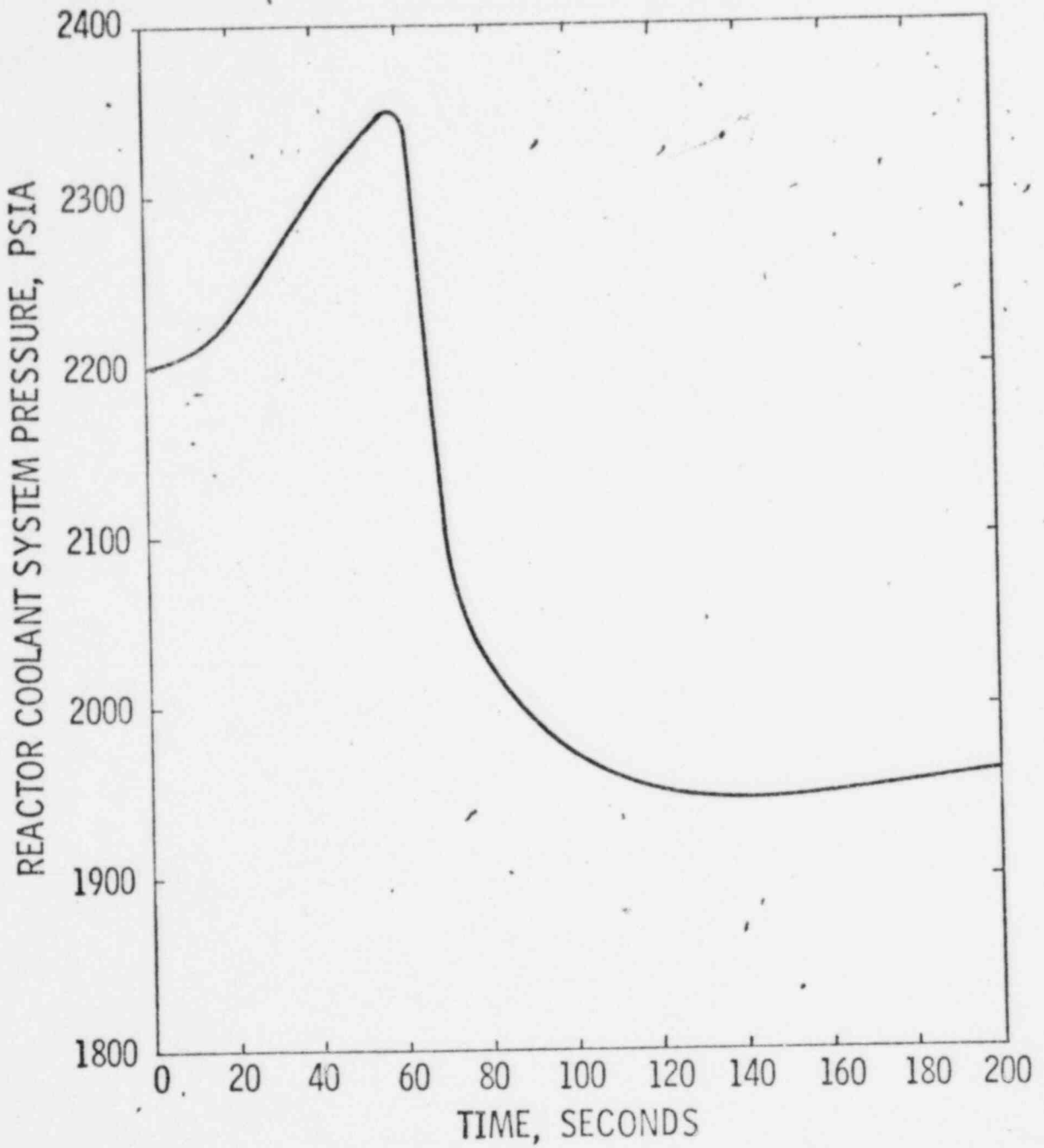


	CEA WITHDRAWAL EVENT FROM 50% POWER CORE AVERAGE HEAT FLUX vs TIME	Figure 7.1-6
--	---	-----------------



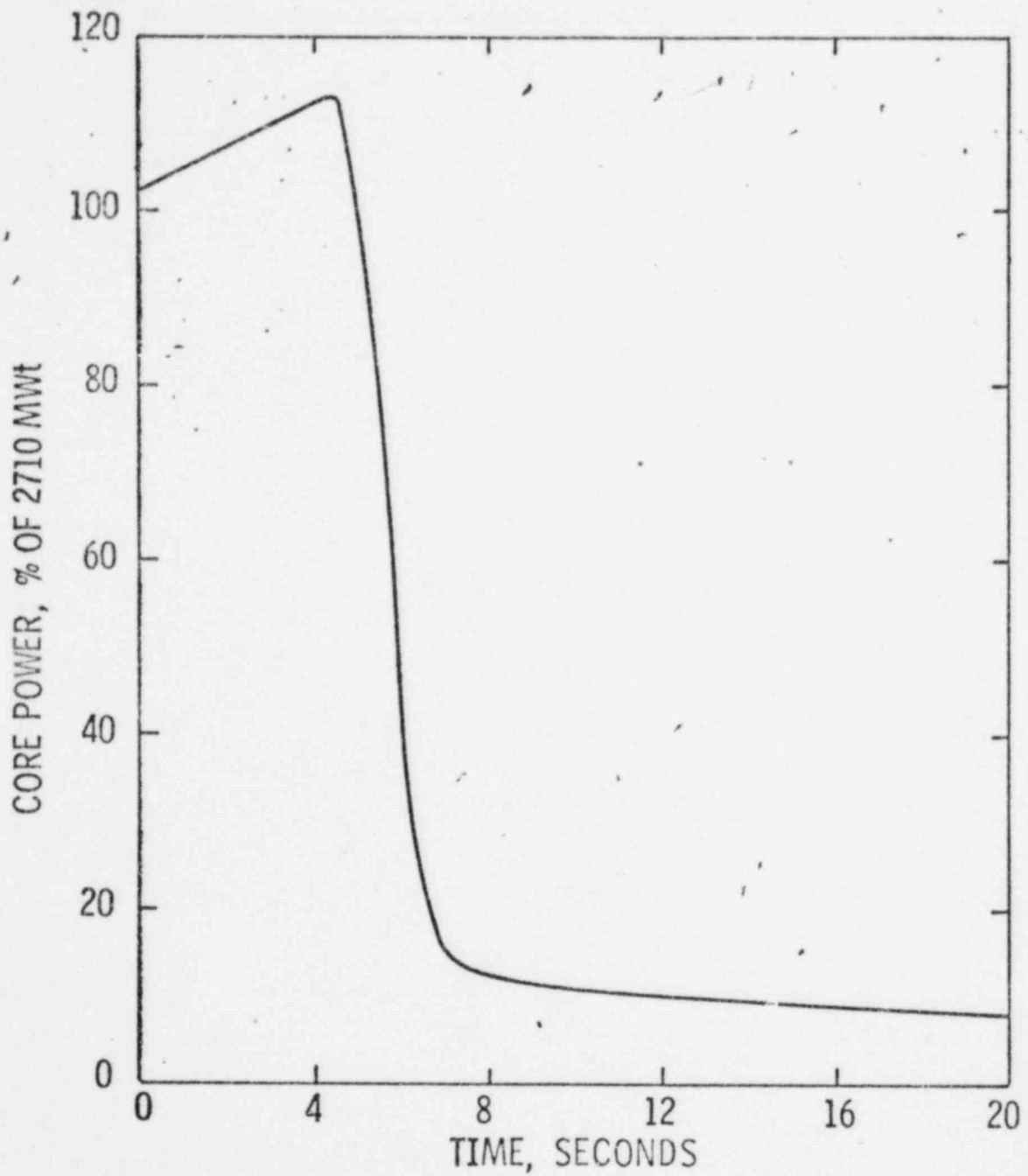
CEA WITHDRAWAL EVENT FROM 50% POWER
RCS TEMPERATURES vs TIME

Figure
7.1-7



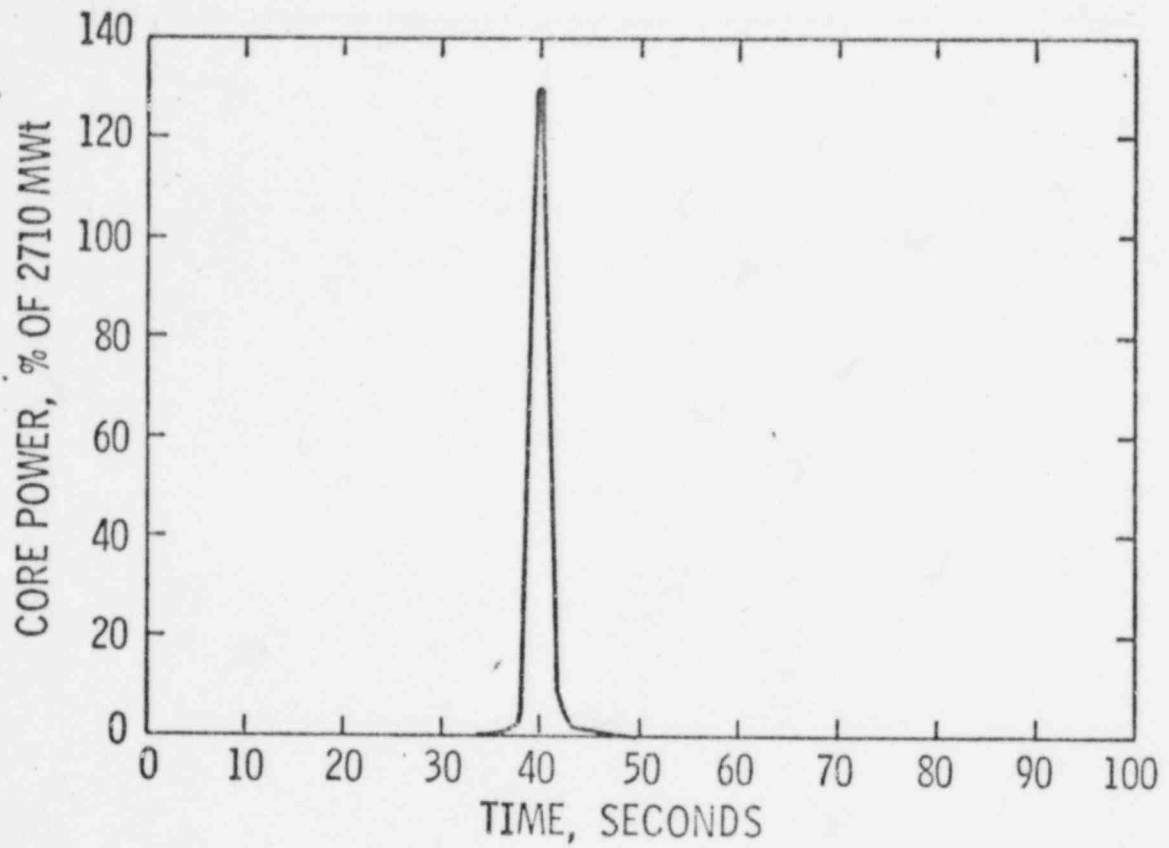
CEA WITHDRAWAL EVENT FROM 50% POWER
RCS PRESSURE vs TIME

Figure
7.1-8



CEA WITHDRAWAL EVENT FROM 102% POWER
CORE POWER vs TIME

Figure
7.2-1



CEA WITHDRAWAL EVENT FROM HZP
CORE POWER vs TIME

Figure
7.2-2

8. CONCLUSIONS

The High Power and Variable High Power Trips and the incorporation of the DNB and LHR ROPM's in generating the DNB and LHR limiting conditions for operation ensures that DNB and CTM SAFDL's will not be exceeded during a CEAW event. The peak linear heat generation rate does not exceed the steady state LHR limit for CEAW transients initiated above 50% of rated power. The steady state LHR limit is exceeded for power levels below 50% of rated power, however fuel centerline temperature melt will not occur. Hence, the results support reclassification of the CEA withdrawal event from the category requiring the TM/LP and ASI trips to the category where sufficient initial thermal margin is built into the LCO's to ensure that DNB and LHR SAFDL's are not exceeded when only the high power or variable high power trips are credited as possible trips to mitigate the event.

9. REFERENCES

1. CENPD-199-P, "C-E Setpoint Methodology", April, 1976.
2. CENPD-107, CESEC Topical Report, July 1974.
3. CENPD-161-P, "TORC Code, A Computer Code for Determining the Thermal Margin of a Reactor Core", July 1975.
4. System 80 PSAR, CESSAR, Vol. 1, Appendix 4A, Amendment No.3, June 3, 1974.
5. Brasfield, H. C., et al, "Recommended Property and Reaction Kinetics Data for Use in Evaluating a Light Water Cooled Reactor Loss-of-Coolant Involving Zircaloy - 4 or 304-SS Clad UO₂", GEMP-482, 1968.
6. SHADRAC, "Shield Heating and Dose Rate Attenuation Calculation", G30-1365, March 25, 1966.
7. W. Engel, Jr., "A User's Manual for ANISN", K-1693, March 30, 1967.

APPENDIX

METHODS USED TO DETERMINE EXCORE DETECTOR RESPONSE DURING A
CEA WITHDRAWAL EVENT

The neutron flux power measured by the excore detectors during a CEA withdrawal event can be calculated by the following expression:

$$\text{Excore Detector Response (t)} = \left\{ \frac{\sum_{i=1}^{\text{NMESH}} \text{AXPD}_i * \text{RSF}_i(t)}{\sum_{i=1}^{\text{NMESH}} \text{AXPD}_i * \text{RSF}_i(t=0)} * \left(1 + \text{TSF} * \Delta T(t) \right) \right\} * P(t)$$

Equation I-1

where:

NMESH = number of axial nodes the core is divided into, which is equal to 20.

RSF_i = rod shadowing factor appropriate for the ith node

AXPD_i = normalized average power in the ith node at t = 0

TSF = temperature shadowing factor (°F)⁻¹

ΔT(t) = T_{in}(t) - T_{in}(t=0)

P(t) = actual core average power at time t.

The rod shadowing factor for a given CEA bank is defined as the ratio of the excore detector response for full insertion of that bank to the excore detector response when all rods are out. The RSF's are determined using detailed two-dimensional power distributions representing the cumulative presence of the various rod banks and the shielding code SHADRAC (Reference 6). In this application SHADRAC calculates fast neutron spectra and fluence for the excore detectors in a three-dimensional system utilizing a moments method solution of the transport equation. The core, vessel internals, vessel and excore detector locations are treated explicitly in the calculation.

The Temperature Shadowing Factor accounts for two temperature dependent effects on the excore detector responses. These are:

1. The effect on detector responses due to varying water density from moderator temperature changes. These are calculated by using computer code ANISN (Reference 7). From ANISN the percent change in detector response per degree change in moderator temperature is calculated.
2. Detector response sensitivity to power shifting due to moderator temperature changes. This is calculated by applying the assembly weighting factors calculated from SHADRAC analyses to the PDQ power maps representative of two moderator temperatures. Again the percent change in detector response per degree change in moderator temperature is calculated.

The total Temperature Shadowing Factor (TSF) is the sum of the above mentioned effects.